International Journal of Future Generation Communication and Networking
Vol.14, No. 1, (2021), pp. 118-144

Analysis Of Delaminated Hybrid Carbon Fiber Composites

[1]Hassan A. Alessa, [2]Steven L. Donaldson
[1, 2]University of Dayton, 300 College Park, Dayton, OH 45469 USA

ABSTRACT:

Fiber reinforced composite materials have been used increasingly in primary and secondary structures in such applications as aircraft, satellites, automobiles, biomedical industries, marine, and sporting goods. This growth is due primarily to the characteristics of composite materials, which include high specific stiffness, high specific strength, and low density. Both carbon and glass fibers are often used as reinforcing fibers, embedded in polymer matrix material. The glass fibers are inexpensive, have high strength to weight ratio, but low stiffness. Carbon fiber is more expensive, but has a high strength to weight ratio and high stiffness.

The delamination between composite layers is one of primary weaknesses in composite material structure. The mode I peeling, mode II shearing, and mixed-mode I/II are the most common delamination fracture crack driving modes between interfaces. Delamination can then lead to a reduction in the structural stiffness. If the structure has compression loading, buckling failure may ensue. The best design approach may find a compromise between less weight and less cost by using a hybrid material approach of both glass and carbon fibers. This research focused on a hybrid materials consisting of both glass and carbon fiber embedded in a polymer matrix, undergoing mode I, mode II, and mix mode I/II static interlaminar fracture. Glass fiber panels, carbon fiber panels, and hybrid panels were fabricated using the wet layup / vacuum bag technique. The non-hybrid all-glass, all-carbon, and hybrid glass/carbon were experimentally characterized by quasi-static testing in load frames. The specimen and material geometries (especially at material interfaces) were analyzed using the finite element method. The program Abaqus was utilized, including the cohesive zone method (CZM). Finally, the resulting fracture surfaces were investigated using a scanning electron microscope. The result showed the fracture toughness values of hybrid material (FG/CF) were between that of fiber glass and carbon fiber. Also, fracture toughness increased due to fiber bridging under static mode I, mode II, and mixed mode I/II.

INTRODUCTION

The application of composite material has been expanding in many structural engineering fields in recent years. This increased use of composite materials is due to their low density, strength, high stiffness, long fatigue life, corrosion resistance and ability to tailor their structural properties. [1].Large structures such as ships, aircrafts, wind turbine blades, cars bodies, and satellites, are fabricated from many materials and parts. Sometimes the structures have failure related to poor design or structural aging. The most common mechanical failure in composite material is delamination, which is separation of the ply layers. Delamination occurs between interfaces because it is the weakest zone in composite materials. The delamination failure modes include mode I, mode II and mix-mode I/II Figure1.1.

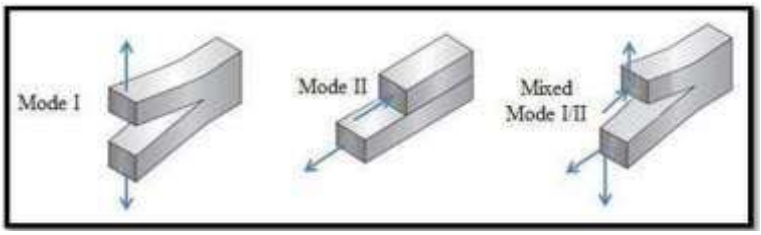

Figure1.1 Mode I, Mode II and Mixed mode I/II. [15]

ISSN: 2233-7853IJFGCN

Composite structures require durability, damage tolerance, long fatigue life cycle, long life, and affordable cost for their light weight. Both carbon and glass fibers are often used as reinforcing fibers, embedded in polymer matrix material. The glass fibers are inexpensive, have high strength to weight ratio, but low stiffness. Carbon fiber is more expensive, but has a high strength to weight ratio and high stiffness. A hybrid fiber approach is a combination more than two fiber types, in an effort to take advantage of each material, to optimize the balance between properties and cost. For example, the incorporation of carbon longitudinal spars in fiberglass wind turbine blades, wind of air craft and sailboats [2, 3, 4, 5].

The primary method to gain information regarding mode I, mode II and mix mode I/II delamination resistance is by experimental mechanical testing. The test responses can then be simulation by using finite element analysis software. This simulation program helps to understand the failure behavior, especially due to mixed model loading. The last step is to examine the resulting fracture surfaces carefully, to help identify energy-absorbing mechanisms that correlate to the mechanical test results.

LITERATURE REVIEW:

The most common delamination fracture failure type studies have been under mode I loading. Many of people had been done mode I fracture on composite material experimental and simulation. The studies considered to serve as an important back ground to the current work are discussed below. In 1982, Whitney, Browning and Hoogsteden conducted mode I experiments with four different materials (AS-1/3502, AS-4/3502, T300/V3778A, AS-1/ Polysulfone, and Bidirectional Cloth) carbon fiber reinforced polymer. They calculated the critical energy release rate by using four methods (Area method, Beam analysis, Empirical Analysis, and Center Notch) with different initial crack. [6]. In 1989, N. Sela,O. Ishai and L.Banks, investigated how adhesive thickness effect on fracture toughness of carbon fiber reinforced plastic between 0.04mm -1.01mm. They found if increase the thickness of adhesive will increase fracture toughness and the adhesive thickness range between 0.1-0.7mm [22].

In 1996, John A. Nairn studied the effect of residual stresses of mode I for double cantilever beam on adhesive and laminate [7]. In 2007, A.J. Brunner, B.R.K. Blackman, P. Davies used alternating 0°/90° layers and increased fiber bridging between two beam by that increased delamination resistance [12]. P.N.B. Reis1a, J.A.M. Ferreira, F.V. Antunes, J.D.M. Costa, C. Capela studied crack initial length on carbon/ epoxy. After they obtained the results of experimental, the specimens were analyze by finite element to creates carve P vs. With different energy release rate and crack length [13]. In 2002, Mehdi Barikani, Hossein Saidpour, and Mutlu Sezen used modified beam theory to study the temperature effect on fracture toughness with different epoxy. They found increasing the temperature decreased fracture toughness [8,9].

In 2008, Solaimurugan, and Velmurugan did mode I fracture with kinds of fiber glass woven and UD with stitched and without stitched. The specimen‟s fiber interface had many orientation designs for UD fiber had 0/0, 30/-30, 45/-45, 60/-60, 90/-90 and 0/90 interfaces and woven had 30/-30, 45/-45 and 90/90 interfaces. Kevlar fiber roving of Tex 175 g/km was the material stitching between two beams. The stitching increase the toughness of specimen three times compare with specimen without stitching [10, 11, 12].

In 1997, Julio F. Davalos did experimental and simulation on hybrid material mode I between wood and fiber-reinforced plastic (FRP) and was using contoured specimen for mode I. The fracture toughness of each wood-wood and FRP-FRP higher than FRP-wood hybrid and he used two method the first one Rayleigh-Ritz and Jacobian derivative method (JDM) [13]. In 1999, Shun-Fa Hwang, Bon-Cherng Shen fabricated mode I specimen hybrid material (carbon fiber and fiber glass). The both beams of mode I specimen had two materials fiber glass and carbon fiber with different fiber orientation and specimen hybrid material (carbon fiber and fiber glass)

ISSN: 2233-7853IJFGCN

obtained higher interlaminar fracture toughness compare with non-hybrid specimen [14]. In 2012 Mohammadreza Khoshravan, Farhad Asgari Mehrabadi fabricated mode I specimen hybrid material of carbon fiber/aluminum and did fracture toughness tested. They used modified beam theory (MBT) and compliance calibration method (CCM) to calculate mode I fracture toughness. They studied how crack length effect on crack failure and they used FEA to analyses stress distribution on long of specimen and width of specimen [15].

In 1998, M. N. Charalambides, A. J. Kinloch and F. L. Matthews investigated on repair carbon fiber reinforce plastic (CFRP) by using scarf joint and applied mode II test experimental and FEA.) [16]. In 2000, P. Compston, P.-Y.B. Jar, P.J. Burchill, K. Takahashi investigated fiber glass reinforced using three different resins and with different fiber volume fracture to compare interlaminated delamination fracture toughness of mode II[31]. In 2003, Stevanovic, Kalyanasundaram, Lowe, and Jar studied how poly (acrylonitrile-butadiene-styrene) (ABS) affected on fracture toughness when mixed with various vinyl-esters (VE) in interface by different mixed ration. ABS was increase the fracture toughness when added with VE less 7% and reduce the fracture toughness when added with VE higher than 7% [64]. In 2006, B.R.K. Blackman, A.J. Brunner, J.G. Williams used specific carbon fiber epoxy (HTA-1200 carbon fiber 113 epoxy resin) for mode II test. In 2007, Masahiro Arai, Yukihiro Noro, Koh-ichi Sugimoto, Morinobu Endo used nano-fiber carbon fiber in specimen inter face with different density for calculate mode II fracture toughness. From the experiments result, increasing density of nano-carbon fiber is increase the fracture toughness [17].

Single leg Bending is one of mixed mode I/II test method Figure1.2.6. In 2003, Gregory D. Tracy, Paolo Feraboli, Keith T. Kedward investigated mix mode single leg four point binding on (RFI) carbon fiber /epoxy laminate of material (IM7-AS4/350-6 hybrid composite system) [18]. In 2007, Cole S. Hamey investigated in Mix mode and fabricated the specimen out of two different kind of wood structures and bind together by epoxy. He used Single Leg Bending (SLB) specimen for experimental test [19]. In 2011, L.F.M. da Silva, V.H.C. Esteves1, F.J.P. Chaves, the specimen fabricated for mix mode of steel/ adhesive / steel. The steel was DIN 40CRMnMo7 and epoxy adhesive was 2015 from Huntsman [20].

MATERIALS AND PROPERTIES

Materials

This research was conducted using composite materials fabricated from S1-HM Unidirectional (UD) fiber glass, EPON Resin 828, EPI-CURE Curing Agent 3223 (Hardener), TORAYCA T300 unidirectional carbon fiber and fluorinated ethylene propylene (FEP) Optically Clear Film made with Teflon.

The fiber glass was donated from AGY-South Carolina. The resin and the hardener were donated from Momentive Specialty Chemicals in Stafford-Texas.

EPON Resin and Curing Agent

The epoxy system used had two main components; first component is the epoxy resin 828 and the second part is curing agent 3223. These two components were equally important since both reacted and contributed to the final structure and properties. The curing agent 3223 was added 10% by weight to the epoxy resin 828 to cure. [1]

Resin

EPON 828, Figure 2.1, is liquid bisphenol A Epichlorohydrin based epoxy resin which contains Phenol, 4,4O - (1-methylethylidene) bis-polymer with (chloromethyl) oxirane [1]

ISSN: 2233-7853IJFGCN

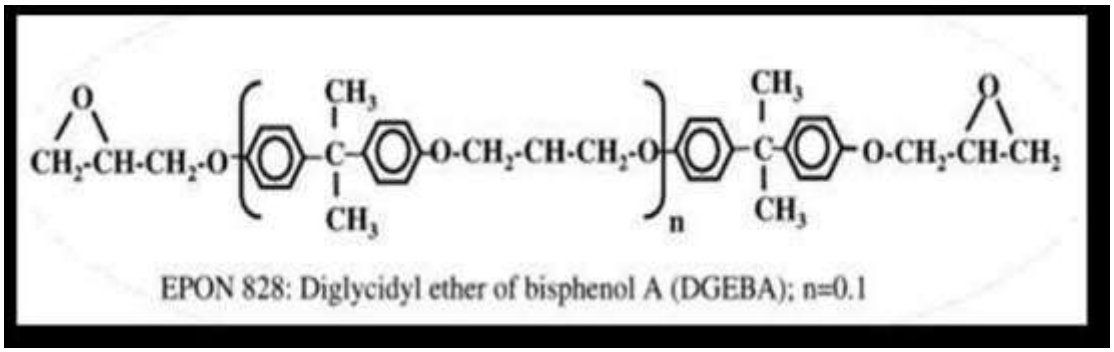

Figure 2.1 EPON 828

And it is one of bifunctional phenolic glycidyl ethers under Diglycidylether of Bisphenol-A (DGEBA), Figure 2.2 DGEBA has two common reactions to ring- opining polymerization and crosslinking, either catalyzed homopolymerization or bridging reactions incorporating a coreactive crosslinking agent into the network (1). These reactions will be discussed in more details in mechanisms section.

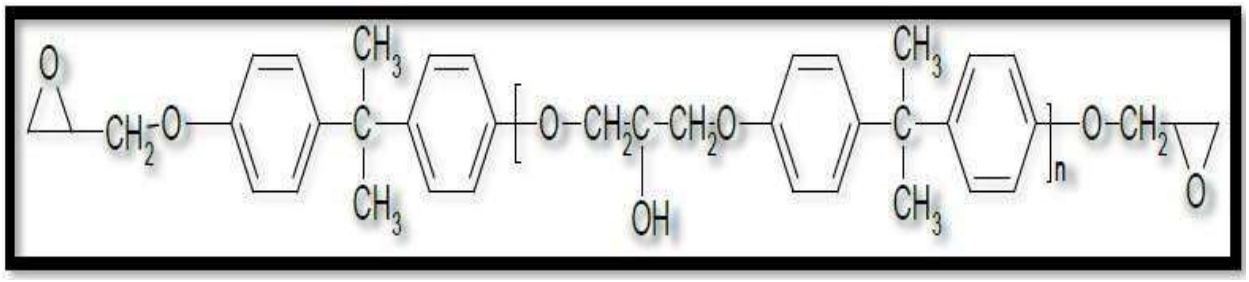

Figure 2.2 Diglycidylether of Bisphenol-A (DGEBA), n = 0, for the derivatives, n > 0.

Curing Agent: EPI-CURE 3223

DIETHYLENETRIAMINE (DETA), N-(2-aminoethyl-1, 2-ethanediamine) is a linear ethyleneamine with two primary and one secondary amine as shown in figure 2. It is a single-component with clear, colorless, and an ammonia-like odor product [4].

DETA is a liquid agent widely used with epoxy resins for fast cures or where room temperature cures are required (Appendix A). Due to exothermic heat of the reaction and the pot life of the catalyzed resin is quite short; this agent is restricted to small casting applications. Although DETA has good properties at room temperature when it is used in curing process (6).

3 PANEL FABRICATIONS AND TENSILE TEST

Panel Fabrication and Sample Cutting:

The simulation using Abaq requires material properties data as input to the9 models. The material properties were collected using tensile test ASTM standard D3039 [4] [5] with strain gage MM (CEA-06-250UW-120). The results were used to calculate , and for the glass and carbon composites used.

They were several steps used to fabricate the specimens for the tensile tests. The fabrication lay-up is shown in Figure 3.1. First, the dry fiber plies were cut into pieces with dimension 19” x 18” (482.6 mm x 457.2mm) for fiber glass. The dimensions for dry carbon fiber pieces were 12” x 12” (304.8mm x 304.8mm). The table surface was cleaned by wiping with acetone. Third, the sealing tape was placed (High Temp Sealant Tape-Yellow) with dimensions of 19.25” x 18.25" (488.95mm x 463.55mm) for fiber glass and for carbon fiber sealing tape dimension 12.25” x 12.25” (311.25 mm x 311.25 mm) was used. Fourth, the non-porous Teflon (234 TFNP non-

ISSN: 2233-7853IJFGCN

adhesive non-porous) was placed over the sealing tape to build a dam structure, which kept the resin contained.

The dimension used for the dry fiber glass was 22" x 21" (558.8 mm x 533.4 mm) and for carbon fiber 15" x 15" (381 mm x 381 mm). Fifth, the resin/harder were well mixed 10:1 by weight, then the epoxy was poured on the Teflon (dam structure). The epoxy was then distributed equally by a squeegee. The first piece of fiber was laid up on Teflon (dam structure), then epoxy was poured on the fiber and was distributed equally by a squeegee. These steps were repeated for the next layers of fibers. The $[0]_T$ fiber glass piece was laid up with one layer for fiber orientation The $[90]_s$ specimens were laid up with two layers having fiber orientation The $[45/-45]_T$ were laid up using two layers with fiber orientation...The $[0_5]_T$ carbon fiber pieces were laid up using five layers for fiber orientation . The carbon $[90_4]_s$ were laid up with eight layers having fiber orientation . Finally, the carbon $[45/-45]_{5s}$ were laid up ten layers for fiber orientation . After the fiber was laid up and resin applied, a layer of non-porous Teflon with thickness 0.003" (0.0762 mm) was placed on top, then an aluminum caul plate with thickness 0.118" (3 mm), after that Teflon with thickness 0.003" (0.0762 mm). Following that, the breather layer was then covered by vacuum bagging with vacuum port and seals the vacuum bagging on the edge by sealing tape and leaks were checked. Finally the vacuum pump was connected to vacuum port and turns on the vacuum pump and keeps it running for 24 hours.

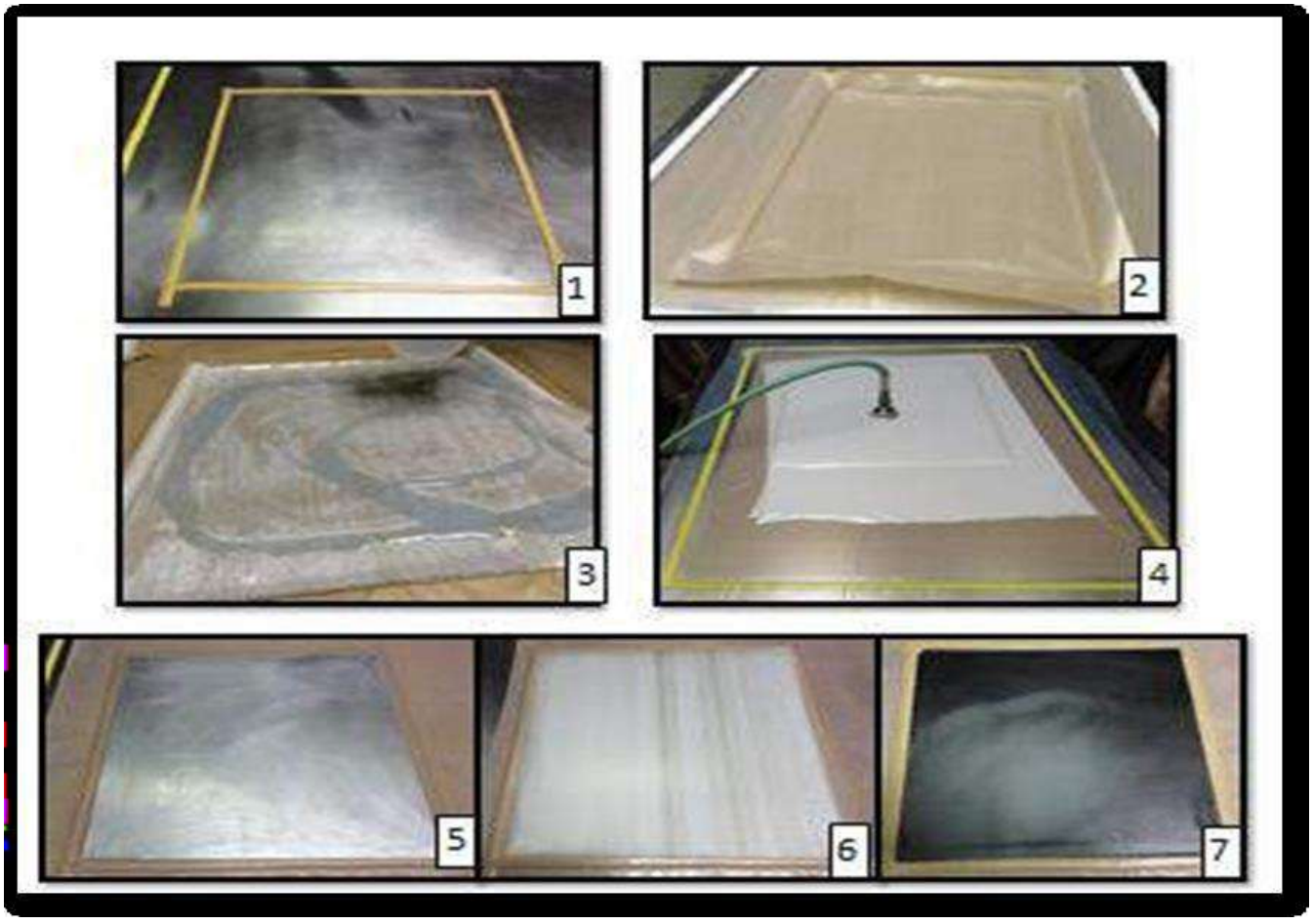

Figure 3.1 Panel Fabrication for Tensile Test and mad tensile specimen

ISSN: 2233-7853IJFGCN

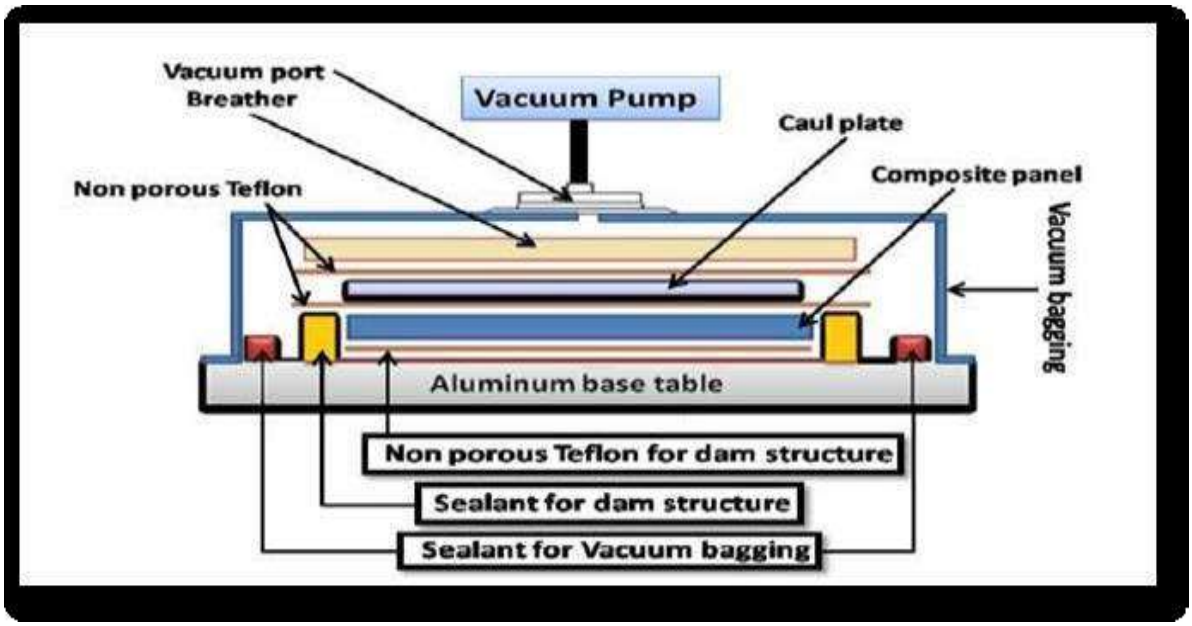

Figure 3.2. (1-7). Panel fabrication steps:
1. Dam structure by sealing tape, 2. Non-porous Teflon, 3. Fiber layup and poured resin, 4. Panel under vacuum for 24 hours, 5. Panel after cure, and vacuum bag and breather removed showing aluminum caul plate, 6. Panel of fiber glass, 7. Carbon fiber panel.

The composite panels were then stored for ten days in room temperature to make certain they were fully cured. Then, the composites panels were then cut with dimension 10" (250 mm) over length for unidirectional and symmetric, but were cutting with dimension 7" (175 mm) over length for unidirectional. The tabs were fixed by super glue with 2.25" (56 mm) length and 0.062" (1.5 mm) thickness for unidirectional panel, 1" (25 mm) length and tab thickness for unidirectional panel. The composite panels were cut into tensile specimens with dimension 0.5" (15mm) x 10" (250mm) x 0.04" (1mm) for fiber orientation unidirectional, tensile specimen with dimension 1" (25mm) x 7" (175mm) x 0.08" (2mm) for fiber orientation 9 unidirectional, and tensile specimen with dimension 1" (25mm) x 10" (250mm) x 1" (25mm) for fiber orientation symmetric. They were cut using a wet diamond saw to avoid micro cracks in the specimen.

Install strain gage on tensile specimen;

The following material and tools were used to install the specimen strain gages: M-Bond 200 adhesive, Teflon tape, sand paper 320-grit, Q-tips, strain gage, tweezers. Figure 3.2 shows the strain gage installation steps: first, clean the gauging area with solvent, such as GC-6 isopropyl alcohol. The solvents have to use one way.[6] The second step is to remove any surface scale and make the surface smooth on the gauging area by sand paper 320-grit. Wiping the gagging area by wetted with M-Prep Conditioner A in one way Figure 3.2.(2-3). After that Wiping the gagging area and scrub with a cotton-tipped wetted with M-Prep Neutralizer Figure 3.2. (3-4). Take the strain gage from package by using tweezers and place on a clean glass plate. Install Teflon tape completed on the terminal and gage. Lift the Teflon tape at angle to glass plate Figure 3.2. (5-7). The specimen angle fiber orientation, install two Teflon tape with strain gage on center of specimen first will be side by side to fiber direction for fiber orientation and

ISSN: 2233-7853IJFGCN

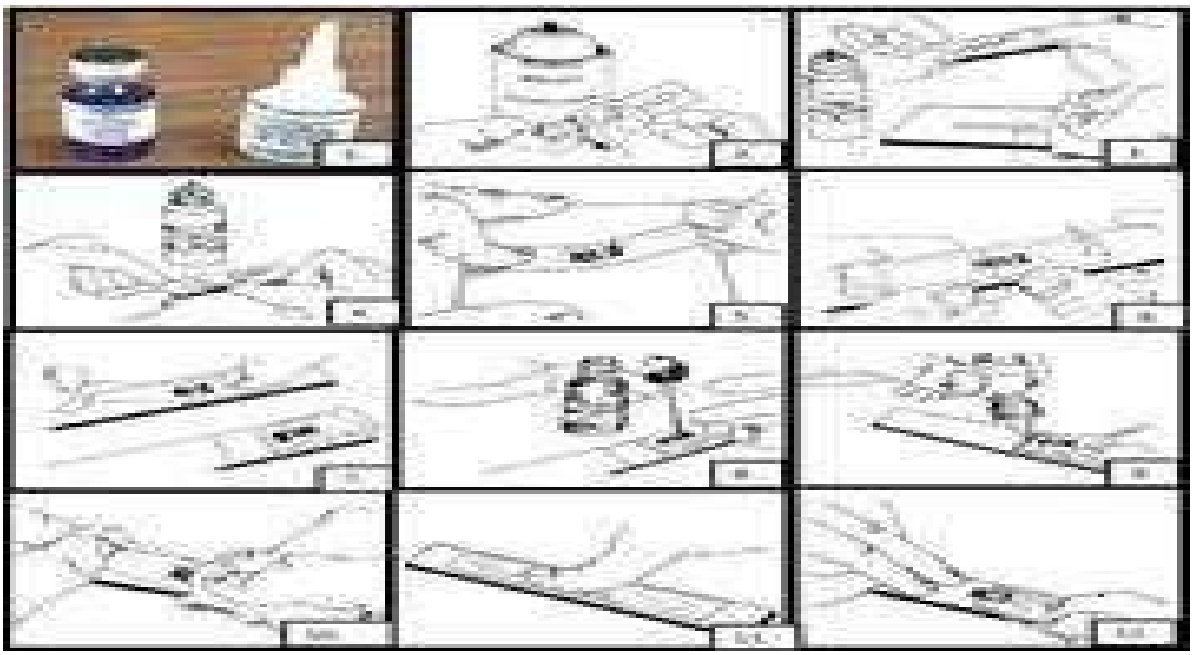

Figure 3.2. (1-12) M-Bond 200 adhesive, (2-12).install strain gage steps [6]

Second one horizontal to fiber direction. The specimen angle fiber orientation was installed Teflon tape with strain gage on center of specimen and vertical with fiber orientation.The specimen angle fiber orientation was installed Teflon tape with strain gage on center of specimen and with angle to fiber orientation Take of one side the Teflon tape from spacemen until reach end of strain gage and strain gage coated by M-Bond 200 catalyst and wait until dry. Put one drab of M-Bond 200 adhesive Figure 3.2. (8-9).The first contact area between spacemen and strain gage. Pull the tape by angle degree and start install Teflon tape with strain gage on spacemen and wipe- out of adhesive Figure 3.2.(4-10). Hold strain gage by thumb to produce the pressure and heat from the thumb on strain gage at least one minute Figure 3.2. (5-11). Remove the Teflon tape my peeling the tape out of spacemen. Figure 3.2. (6-12).

Soldering the wire with strain gage connector:

Warm up the solder iron and clean up the head of solder iron and make sure the solder tip clean too by pass the solder iron tip on a wet sponge until get it shines.

Tin the head of solder iron, strain gage connector, and the head of wire by lead (tinning is coating a head of soldering tip by thin layer of lead). Tinning helping the heat flow from the tip of soldering to between the components you are soldering.

Heat the wire by head of the tip until reach the same the temperature and try to connect the wire on strain gage connector and feed them by lead. Remove the lead first after that the solder tip. Install small piece of masking tape on wire and end spacemen toake sure the connecting area between wire strains gages do not move to avoid strain gage damaging. Repeat this processing with all spacemen.

Tensile testing

Static tensile tests were conducted following the ASTM standard D3039 and D 3039M-08 [7] using the specimens with fiber orientation, fiber orientation, and fiber orientations, as shown in Figure 3.4.Five samples from each, and fiber orientation and different material (fiber glass and carbon fiber) of the six panels were tested to calculate young's modulus, and for fiber glass and carbon fiber.

ISSN: 2233-7853IJFGCN

Table 3.4 .1 The average of tensile test specimens dimensions**:**

	Width (b)	Length (L)	Thickness (h)	Area (A)
Carbon fiber unidirectional	0.54" (13.57mm)	10" (250mm)	0.04" (1.03mm)	0.0177" (13.91mm)
Carbon fiber unidirectional	1.08" (27.34mm)	7" (175mm)	0.09" (2.27mm)	0.095" (0.095mm)
Carbon fiber symmetric	1.03" (20.91mm)	10" (250mm)	0.079" (1.61mm)	0.0813" (33.57mm)
Fiber glass unidirectional	0.53" (13.5mm)	10" (250mm)	0.04" (0.98mm)	0.020" (13.17mm)
Fiber glass unidirectional	1.028" (26.121mm)	7" (175mm)	0.073" (1.84mm)	0.075" (48.169mm)
Fiber glass symmetric	1.015" (25.77mm)	10" (250mm)	0.076" (1.93mm)	0.077" (49.62mm)

Static tensile tests were conducted using a screw-driven mechanical test frame, Instron 5500R, as shown in Figure 3.4(1). The first step was that the specimens were installed in the grips and the strain gage wires connected to the strain gage input card of the scanner panel (Vishay, Model 5100B Scanner, System 5000) Figure 3.4.(2-4). Load and displacement were reset, and the test was started at a displacement rate of 2mm/min [0.05in/min]. After that, the test was stopped and repeated with the other specimens, as shown in Figure 3.4. (5-8).

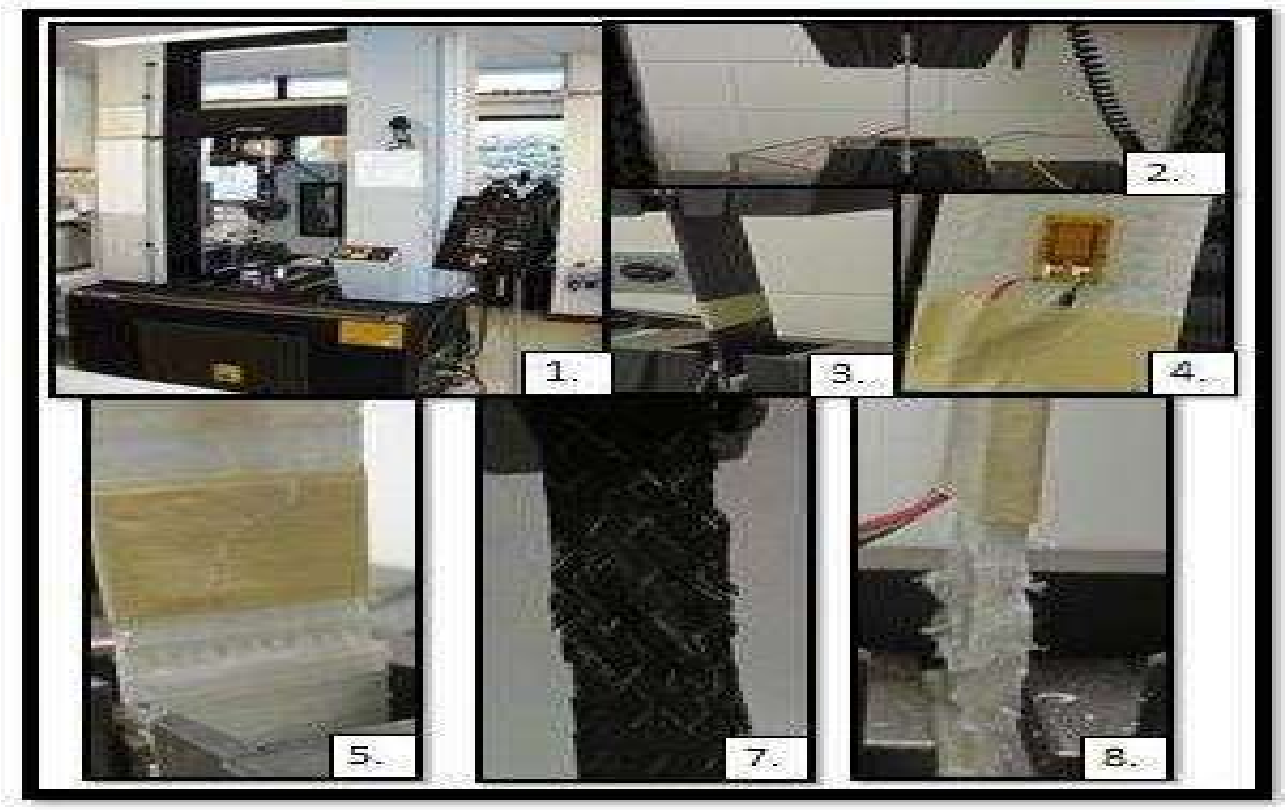

Figure 3.4.(1-8)
(1) Instron 5500R frame, (2-4) specimen was installed in upper and lower grips of Insttron machine , (5-8) specimens after tinsel tests

ISSN: 2233-7853IJFGCN

Calculations

Table 3.5.1 Property of fiber glass-S1-HM UD / Epon 828 epoxy composite

FG-S1-HM UD TENSILE MODULUS		
	5.431 Msi	37448.305 Mpa
Tensile strength	2207.5 lb.	9822.804 N
	1.712 Msi	11806.780 Mpa
Tensile strength	402.76 lb.	1792.178 N
	0.308 Msi	2654.051 Mpa
Tensile strength	662.86 lb.	2949.553 N
	0.175	

Property of carbon fiber T300/ Epon 828 epoxy composite

CF-T300		
	25.821 Msi	178031.971 MPa
Tensile strength	4829.967 lb.	21492.101N
	0.956 Msi	6596.138 MPa
Tensile strength	349.92 lb.	1557.053 N
	0.384 Msi	2124.237 MPa
Tensile strength	3779.12 lb.	16816.106N
	0.373	

4. PANEL FABRICATION AND TESTS OF MODE I, MODE II AND MIXED MODE I/II

Panel Fabrication:

The overall goal of this paper is to discuss the developments of hybrid DCB for mode I, hybrid ENF for mode I, and mix mode I/II. It will also address the key tasks involved in the development of all three types of composites material such as: (1) Carbon-fiber/Epoxy composite (2) Glass-fiber/Epoxy and (3) Hybrid (Carbon and Glass fibers) composites. The development of a reliable, and , analysis of hybrid DCB, hybrid ENF, and single leg bending (ASLB). The first step in this research was to match bending stiffness of fiber glass and carbon fiber for hybrid DCB, ENF, and ASLB.

ISSN: 2233-7853IJFGCN

Table 4.1 Matched bending stiffness of carbon fiber and fiber glass**:**

	Thickness m	S1-HM UD TENSILE MODULUS EI	TORAYCA T300 EI	Thickness m	
	1.00E-03	50.8	8.466	0.0001	
	2.10E-03	106.68	1.69E+01	0.0002	
	2.20E-03	111.76	25.4	0.0003	
	2.30E-03	1.17E+02	33.866	0.0004	
2 layers	2.40E-03	121.92	42.333	0.0005	
	2.50E-03	1.27E+02	50.8	0.0006	
	2.60E-03	132.08	59.266	0.0007	
	2.70E-03	137.16	67.7333	0.0008	
	2.80E-03	142.24	76.2	0.0009	
	2.90E-03	147.32	84.666	0.001	
	3.00E-03	152.4	93.133	0.0011	
	3.10E-03	157.48	101.6	0.0012	
	3.20E-03	162.56	110.066	0.0013	
	3.30E-03	167.64	118.533	0.0014	
	3.40E-03	172.72	127	0.0015	8 layers
	3.50E-03	177.8	135.466	0.0016	

They were several steps necessary to fabricate the tensile test specimens. First, the dry glass fiber plies were cut into pieces with dimensions 19” x 18” (482.6 mm x 457.2mm). The dimension for cutting the dry carbon fiber was 12” x 12” (304.8mm x 304.8mm). Second, the surface of tje table was cleaned from remaining resin or dirt and wiped using acetone. Third, sealing tape with dimensions 19.25” x 18.25" (488.95mm x 463.55mm) for fiber glass, and tape dimension 12.25” x 12.25” (311.25 mm x 311.25 mm) were used for carbon fiber were placed on the tool. Fourth, the non-porous Teflon sheet with dimensions 22” x 21” (558.8 mm x 533.4 mm) for glass fiber and 15” x 15” (381 mm x 381 mm) for carbon fiber was laid up over the sealing tape to build a dam structure to keep the resin contained. Fifth, the resin / hardener were well mixed with 10:1 (by weight) and the epoxy was poured onto the Teflon (dam structure). The epoxy was then distributed equally using a squeegee. The first piece of dry fiber was laid up on the Teflon (dam structure), then epoxy was poured on fiber and was distributed equally by a squeegee. These steps were repeated for the next layers of fibers Fiber Glass Panel The dry glass fiber panels had two distinct sides, as shown in Figures 4.1 and 4.2. The side shown in Figure 4.1 had a small amount of 90° cross weave placed to increase the handing capacity of the primarily unidirectional tows. This face was designated as the 90-face. The opposite face is shown in Figure 4.2.2. It shows the back face of

ISSN: 2233-7853IJFGCN

the layer, with the V cross- weaves. This face was designated as the V-face. Therefore, there were three possible combinations of planes for crack growth between glass fiber layers, so the panel fabrication needed to account for this. The first type of fiber glass orientation was denoted as 90/V. Two pieces of fiber glass were laid up with 90 directions facing down Figure 4.2.1. Then, the Teflon insert (0.005") was laid up on top second layer. After that, two more layers were laid up with 90 directions facing down.

Figure 4.1 Fiber glass 90

Figure 4.2 Fiber glass V

Figure 4.3 Carbon fiber T300

The second model of fiber glass orientations called for 90/90 at the center interface. Two wet pieces of fiber glass were laid up with 90 directions facing up and V directions facing down. Then, the Teflon insert 0.0005" (0.0127mm) was laid up on top second layer. After that, two more wet layers were laid up with 90 directions facing up and V direction facing down. The third model of fiber glass orientations called for V/V at the center interface. Two wet pieces of fiber glass were laid up with V directions facing up and 90 directions facing down. Then, the Teflon insert 0.0005" (0.0127mm) was laid up on top second layer. After that, two more wet layers were laid up with V directions facing up and 90 directions facing down.

Carbon Fiber Panel

The carbon fiber plies did not have any preferred „face" or side, as shown in Figure 4.3. They were laid up with ten layers, with distributed epoxy equally on each piece between layers. Then the Teflon insert was laid up on top of the ten layers of carbon fiber. After that, another ten layers of carbon fiber laid up on top Teflon insert.

Hybrid of Carbon Fiber and Fiber Glass Panel:

They are two types of fiber orientation with the hybrid specimens. The first type of hybrid is referred to as carbon fiber/90 glass fiber. First, two layers of fiber glass with the V direction facing down and 90 facing up were laid down and saturated with resin. The Teflon insert was then laid up on fiber glass 90 faces. After that, ten layers of carbon fiber were laid up.

The second model of hybrid specimens is referred to as carbon fiber/V glass fiber. Two wet layers of fiber glass the 90 directions facing down were laid up, with the V surface facing up. The Teflon insert was then laid up on fiber glass V face. After that, ten wet layers of carbon fiber were laid up.

After the wet fiber plies were laid up, they were covered by a non-porous Teflon 3 mil sheet 3, followed by the aluminum plate, Teflon sheet, breather layer, and vacuum bag. The vacuum bag was connected to a central vacuum port and the vacuum port connected to the vacuum pump. The vacuum pump was run for 24 hours. Following that, each panel was stored for ten days to get full curing. A total of twelve panels were fabricated:

three of fiber glass panels, three carbon fiber, and six hybrid panels.

ISSN: 2233-7853IJFGCN

Sample Cutting

After ten days (for full cure) the panels were cut into specimens. The fiber glass panel Figure 4.4.4.(1) was cut into two pieces for Mode I and Mode II specimens. The Mode I piece has size 8.5" (469.9mm) x 6.25" (158.75mm), and the Mode II piece had a size of 8.5" (469.9mm) x 6.25" 8.25" (209.55mm). The panels edges were parallelized by using a roller sander, as shown in Figure 4.4.4.(5). The carbon fiber Figure 4.4.4.(2) and hybrid Figure 4.4.4.(3) panels were also cut into two pieces, as shown in Figure 4.4.4.(4). The Mode I pieces for both the carbon and hybrid were 12" (304.8mm) x 5.25" (133.35 mm)], and the Mode II pieces for both carbon and hybrid were 12" (304.8mm) x 6.72" (184.15mm)]. The specimen edges were also parallelized.

The dimensions of the Mode I fiber glass specimens were 7" (177.8mm) x 1"(25.4mm). The Mode II glass fiber specimens were 8" (203.2mm) x 1" (25.4) as shown in Figure 4.4.1. The carbon fiber and hybrid Mode I specimens dimensions were 5" (127mm) x 1"(25.4mm), and 7" (177.8mm) x 1" (25.4) for the Mode II specimens, as shown in Figure 4.4.2. The hybrid mixed-mode specimen dimensions were 8" (203.2mm) x 1"(25.4mm) as shown in Figure 4.4.3. The mode I specimen had 2.5" Teflon insert implanted in the panels, whereas the Mode II and mix-mode had a 2" Teflon insert.

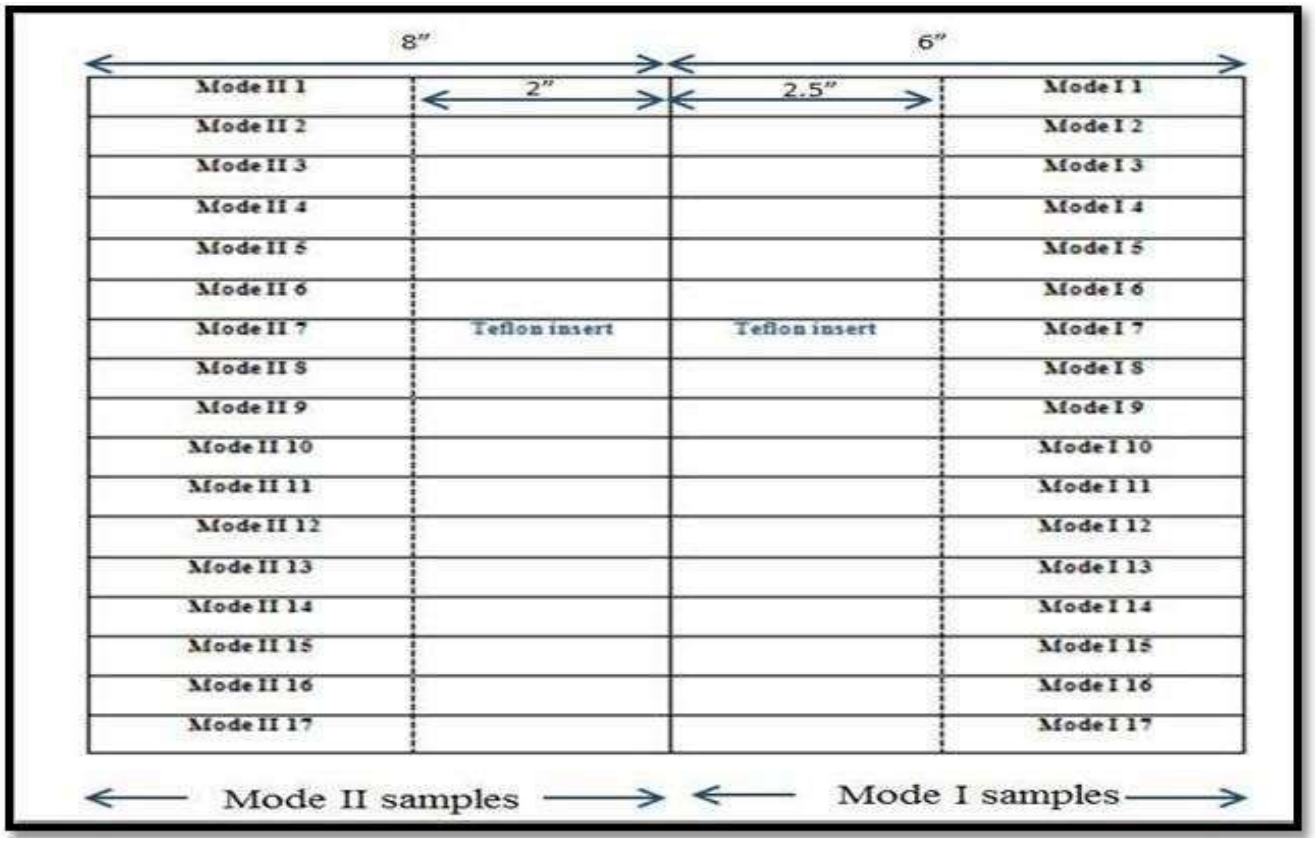

Figure 4.4.1 Fiber glass panels dimension.

ISSN: 2233-7853IJFGCN

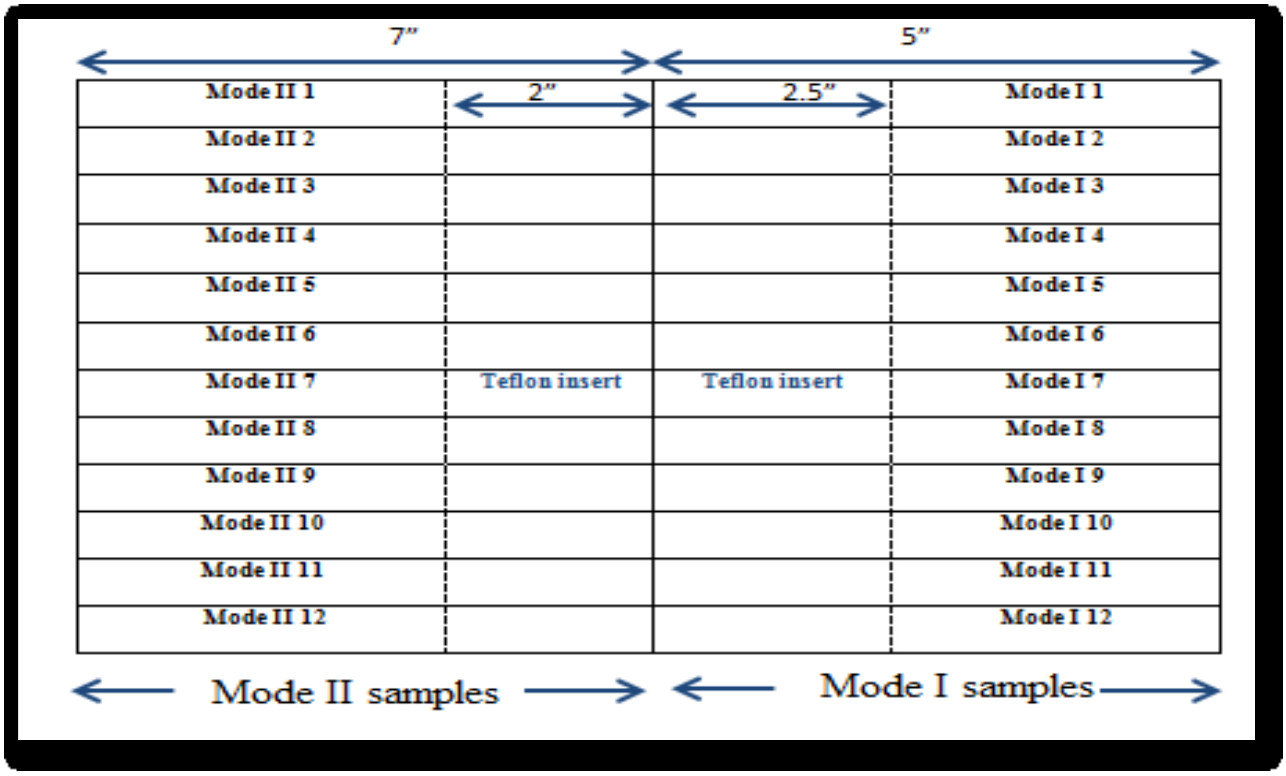

Figure 4.4.2 Carbon and hybrid fiber panels dimension.

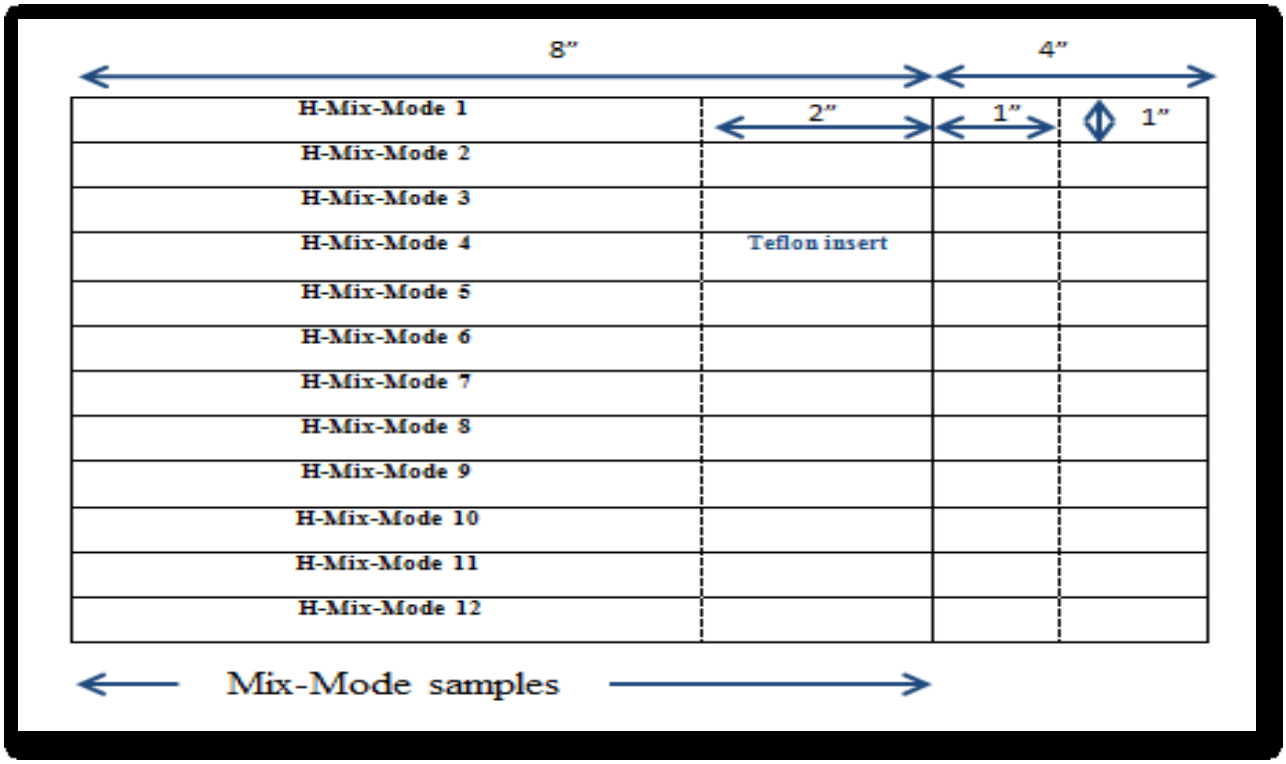

Figure 4.4.3 Hybrid mix-mode panels dimension.

ISSN: 2233-7853IJFGCN

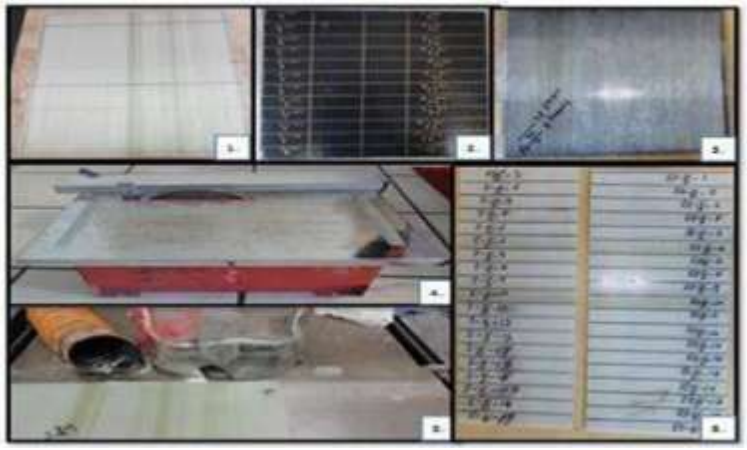

Figure 4.4.4. (1-6) 1. Fiber glass panel, 2. Carbon fiber panel, 3. Hybrid (CF/FG) panel, 4. Wet diamond saw, 5. Parallelizing the panels, 6. The panels were parallelized and ready for cutting to make specimens.

Mechanical Testing

This research was conducted under static test conditions for mode I (Double Cantilever Beam, DCB), mode II (End Notched Flexure, ENF) and mixed-mode I-II (Single Leg Bending, SLB). The goal of the project was to study the interlaminar fracture toughness of hybrid composite materials.

Sample's Preparation for Mechanical Testing

Specimens for mode I, mode II and mix-mode were prepared for mechanical testing. Mode I specimen preparation followed ASTM D5528 standard [8], each sample edge was filed with 600 grit sand paper to produce smooth edges. Next, the specimen dimensions of spacemen length, width and thickness were recorded. The bonding regions of aluminum T- tabs were filed by sand paper until shiny. T-tabs were bonded (using cyanoacrylate "super glue") on each side of the specimen at the ends containing the Teflon insert. The spray gun shown in Figure 4.5.1.1(1) was used to coat mode I specimens just ahead of insert side by using water based Polly Scale white paint, as shown in Figure 4.5.1.1(2) to visualize the crack delamination growth. Ten vertical lines were marked on each specimen at five millimeter length intervals, as shown in Figure 4.5.1.2.

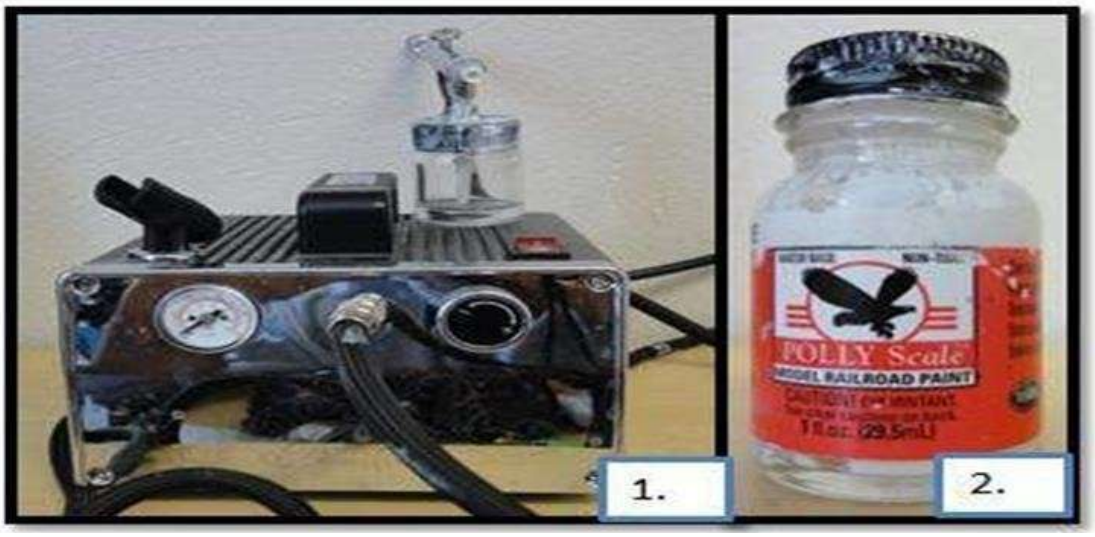

Figure 4.5.1.1 Spray paint gun and air pump, (2) Polly Scale white paint water base

ISSN: 2233-7853IJFGCN

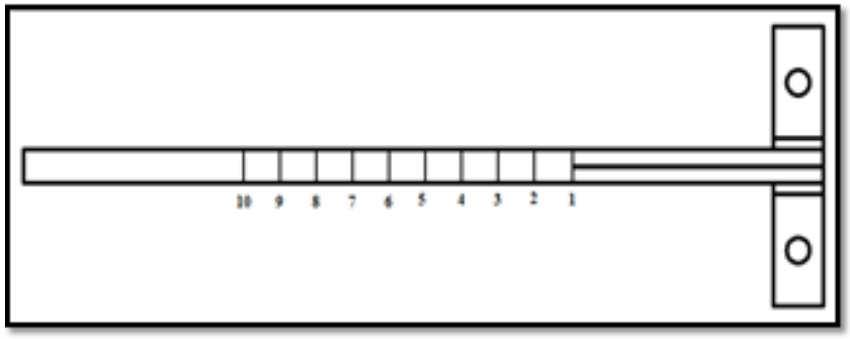

Figure 4.5.1.2 The DCB specimen marked with vertical marks every 0.2" (5mm) starting at insert.

Mode II preparation, each sample edges was filed by 600 grit sand paper to have smooth edge. Second steps get the dimension of spacemen length, width and thickness. The spray gun was used to coat mode I specimen just ahead of insert side by using (water based Polly Scale white paint).

The mode II specimens were marked with vertical two marks the first end insert the second one after the insert 1.2" (30.48mm).

Mix-mode preparation, each sample edges was filed by 600 grit sand paper to have smooth edge. Second steps get the dimension of spacemen length, width and thickness. The spray gun was used to coat mode I specimen just ahead of insert side by using (water based Polly Scale white paint).

The mix-mode specimens were marked with vertical two marks the first end insert the second one after the insert 1.2" (30.48mm) and cut one of ENF a leg 1.5" (38.1mm) length to make SLB.

DCB Mode I Fracture Static Test:

The Mode I Double Cantilever Beam (DCB) test was developed to measure the interlaminar fracture toughness under peeling stress. The mode I testing conducted in this study was using the unidirectional fiber (UD) laminates, except with the minor cross-stitch as discussed previously. The fibers directions were along the long axis of the specimens Figure 4.5.2.1.The mode I static testing was conducted following ASTM standard D5528 [8]. Five samples of each of six design were tested to calculate G_{IC}, the mode I interlaminar fracture toughness.

Table 4.6.2 The dimensions (average) of DCB specimen:

Mode I	Width b	Length L	Thickness h	Initial delamination length a_o
FG-90-V	1.034" (26.26mm)	7" (177.8mm)	0.174" (4.428mm)	2.5" (63.5mm)
F.G-90/90	1.03" (26.14mm)	7" (177.8mm)	0.181" (4.59mm)	2.5" (63.5mm)
F.G-V/V	1.02" (25.9mm)	7" (177.8mm)	0.183" (4.66mm)	2.5" (63.5mm)
CF	1.04" (26.4mm)	7" (177.8mm)	0.234" (5.9436mm)	2.5" (63.5mm)
H-CF-FG-90	1.03" (26.11mm)	5" (127mm)	0.184" (4.66mm)	2.5" (63.5mm)

ISSN: 2233-7853IJFGCN

H-CF-FG-V	1.03" (26.13mm)	5.5" (139.7mm)	0.19" (4.76mm)	2.5" (63.5mm)

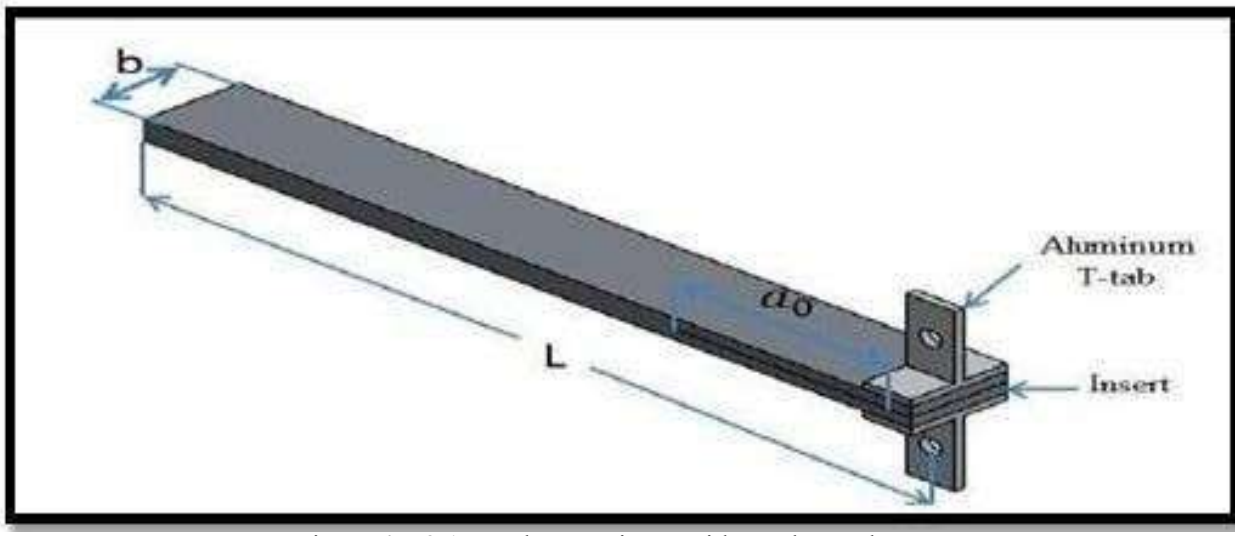

Figure 4.5.2.1. Mode I specimen with T-tab attachment

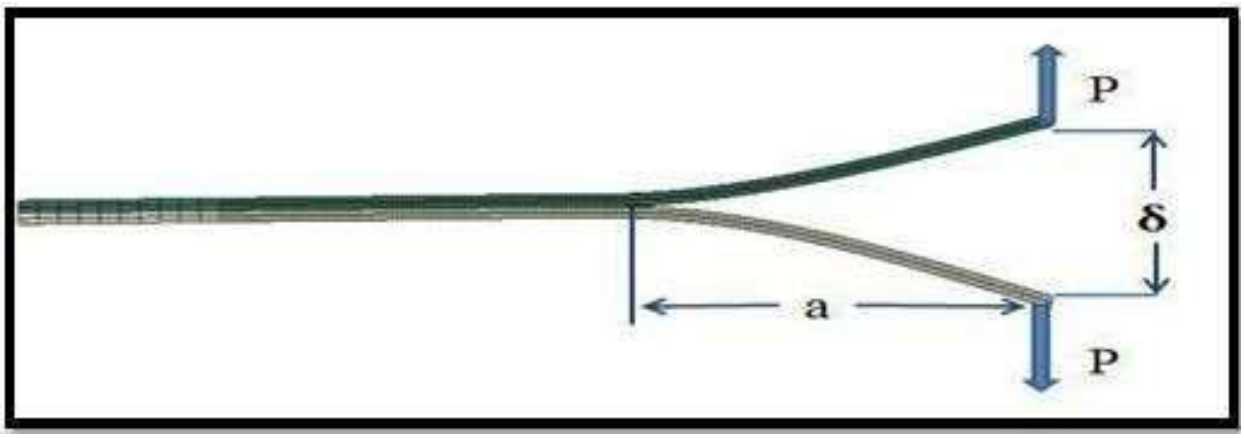

Figure 4.5.2.2 The DCB specimen is in open mode of the static test.

An Instron 5500R Model 1123 was used to provide the mechanical force for the mode I tests. It was a screw-driven mechanical test frame. It was measuring the load P, and opening distance, Figure 4.5.2.2. The max load of load cell used was 200 lb. The speed displacement rate was 0.1"/min. during the test. A magnifier and bright light source were employed to follow the crack propagation. When the crack propagated and arrived to a mark point, a custom tapping device was used to digitally mark on curve (P vs. δ) to calculate G_{IC}.

In order to conduct the tests, first, each the mode I specimen was attached to the Instron machine by using two pins Figure 4.5.2.3.(1-2). Second, the load and displacement were reset. Note this test did not require mechanically precracking the specimen before the test, because the thin Teflon inserts 0.5 mil was used according ASTM Standard D5528 [8]. Testing was then conducted at a displacement rate 0.1"/minute while the crack propagation was monitored using magnifier and bright light source. The tapping device was taped 10 times, each time when the crack reaches a vertical line during the crack propagation.

ISSN: 2233-7853IJFGCN

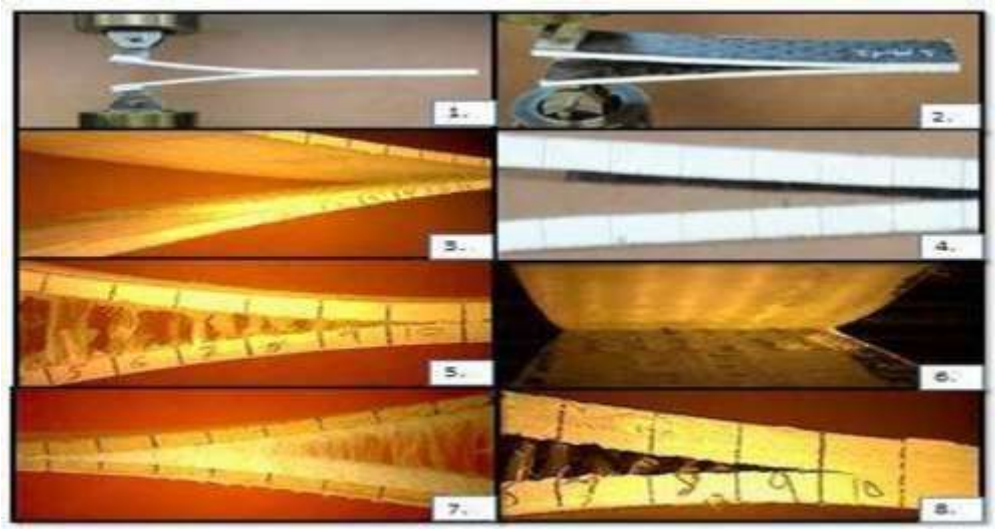

Figure 4.5.2.3
(1-2)Specimen installed in Instron machine by T taps, (2,4)The carbon fiber, (3) fiber glass V-V, (5) fiber glass 90-90, (6) H-CF/FG-V, (7) fiber glass 90-V, (8) H-CF/FG-90

The FG and CF specimens were attached to the Instron machine by pins in the T-tab as shown in Figure 4.5.2.3 (1-2). The carbon fiber fracture and fiber glass V-V did not show fiber bridging. Figure 4.5.2.3 (3-4). The fiber glass 90-V and fiber glass 90-90 did show fiber bridging. Figures Figure 4.5.2.3 (5) (7). The fracture area of the hybrid H- carbon fiber/ fiber glass V-V did not have fiber bridging, but the carbon fiber side of the specimen appeared to be covered with the fiber of the fiber glass. Figure 4.5.2.3 (6). The hybrid H-carbon fiber/ fiber glass 90 showed fiber bridging Figure 4.5.2.3 (8).

Mode II-ENF Static Test:

The Mode II End Notch Flexure (ENF) test was designed to measure the interlaminar shear fracture energy under the shearing mode. The mode II test used in this study was conducted using the unidirectional fibers (UD fibers), except for the slight cross-stitch used to hold the UD fiber tows together, as discussed previously. The fibers were aligned with the length of the specimen. The mode II static test was conducted following the ASTM draft standard by Davidson [9]. Five samples mode II of each six of designs were tested to calculate G_{IIC} mode II interlaminar shear fracture toughness. The specimen is shown in Figure 4.6.3.1.

Table 4.6.3 The dimensions (average) of ENF specimens

Mode II	Width b	Length L	Thickness h	Initial delamination length a_o
FG-90-V	1.03” (26.26mm)	8” (203.2 mm)	0.174” (4.43mm)	2” (50.8mm)
F.G-90/90	1.03” (26.14mm)	8” (203.2 mm)	0.18” (4.43mm)	2” (50.8mm)
F.G-V/V	0.97” (24.67mm)	8” (203.2 mm)	0.18” (4.60mm)	2” (50.8mm)

ISSN: 2233-7853IJFGCN

CF	1.04” (26.4mm)	8” (203.2 mm)	0.234” (5.94mm)	2” (50.8mm)
H-CF-FG-90	1.02” (25.87mm)	7” (177.8mm)	0.181” (4.60mm)	2” (50.8mm)
H-CF-FG-V	1.03” (26.19mm)	7” (177.8 mm)	0.189” (4.79mm)	2” (50.8mm)

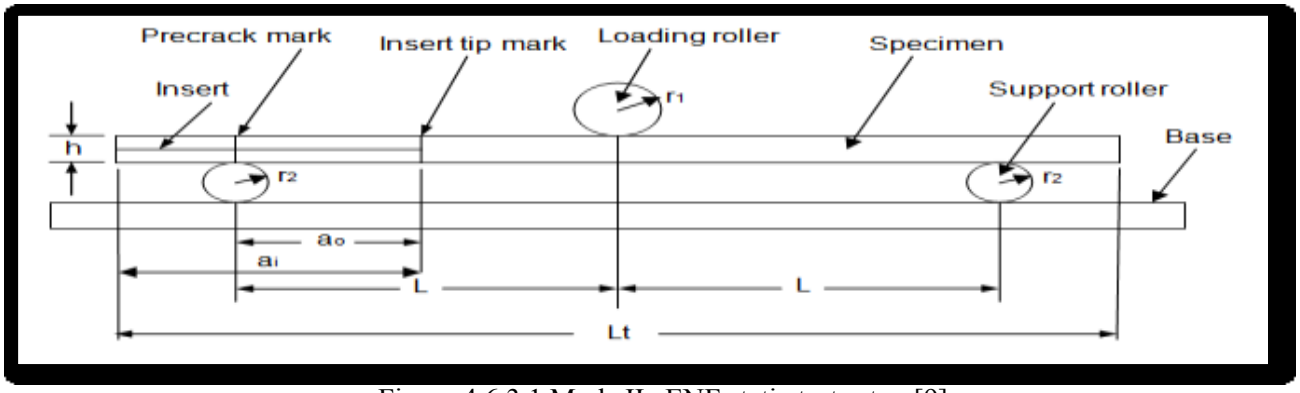

Figure 4.6.3.1 Mode II –ENF static test setup [9]

A screw-driven Instron mechanical test frame was used for the three point bending flexural test required to calculate mode II fracture energy. It measured the load and opening displacement. The maximum load of the load cell was used was 500 lb. The displacement rate was 0.025 in/min. During the test, a magnifier and bright light source were used to follow the crack propagation.

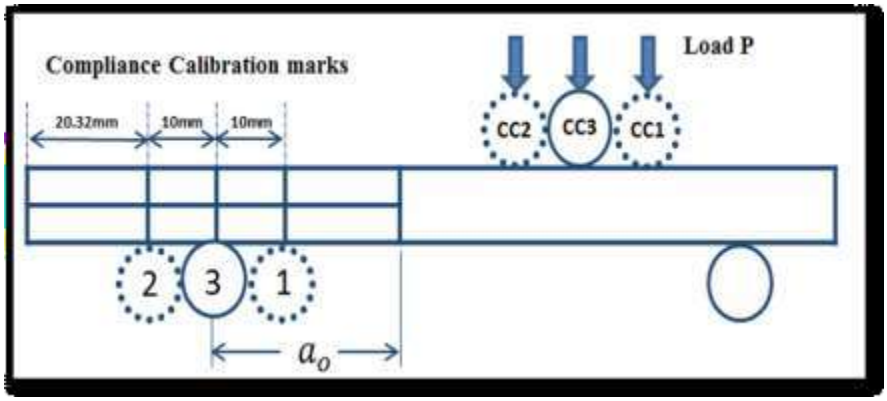

Figure 4.6.3.2 The three positions of CC and the fracture test marks.

The ENF static test was conducted using two main steps. Precracking was not necessary for the specimen since it had a 0.5 mil thickness Teflon insert. Three compliance calibration (CC) runs were made before each actual test. Each specimen was marked with four marks by a thin vertical line, as shown in Figure 4.6.3.2. The locations of the vertical lines were as follows, as shown in Figure 4.6.3.2: line labeled 1 was 1.7” (40.32 mm) from the left edge of the specimen, line labeled 2 was 0.8” (20.32 mm) from the left edge, the line labeled 3 was 1.2” (30.32 mm) from the left edge of the specimen. The fourth line (at the right edge of the dimension a_0 in Figure 4.6.3.2) was at the end of the Teflon insert, which was 2” (50.8 mm) from the end of the specimen.

ISSN: 2233-7853IJFGCN

Compliance Calibration Processing

Each specimen was tested in three point flexure. The dimension in Figure 4.6.3.1 were L = 2 inches (50.8mm), L_t = 8inches (203.2) ai =2 inches (50.8mm) a_0 =0.8 inches (20.32mm) . During the compliance calibration, each specimen was loaded to 50% of maximum load (without crack propagation), followed by complete unloading. The specimen was then shifted to the second position for CC2 and the process repeated. The specimen was then shifted to the third position for CC3, where the specimen was loaded to maximum failure load causing crack propagation. The load P and the displacement δ during CC1, CC2 and CC3 were recorded.

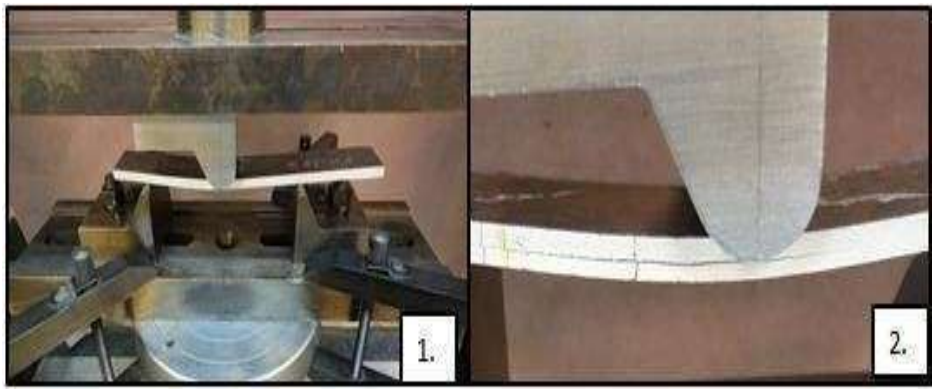

Figure 4.5.6.3.3Carbon fiber specimen for mode II set on flexure during mode II test, (2) The crack propagate until end of the load area from upper roller 0.8" (20.32mm)

The Mode II specimens testing resulted in specimens that were still fully joined, since the crack did not propagate fully along the length of the specimens, as designed. Therefore, the amount of fiber bridging could not be ascertained by looking at the specimen edges. Figure 4.5.6.3.3.

Mixed-Mode I / II

The Single Leg Bending (SLB) test was designed to test the interlaminar mix-mode I-II critical fracture energy. The mix-mode SLB tests conducted in this study were tested using the unidirectional fibers (UD fibers) specimens. The fiber directions were along the length of the specimen. The mixed-mode static test was done following the Single Leg Bending (SLB) specimen by Szekrenyes an Uj [10].

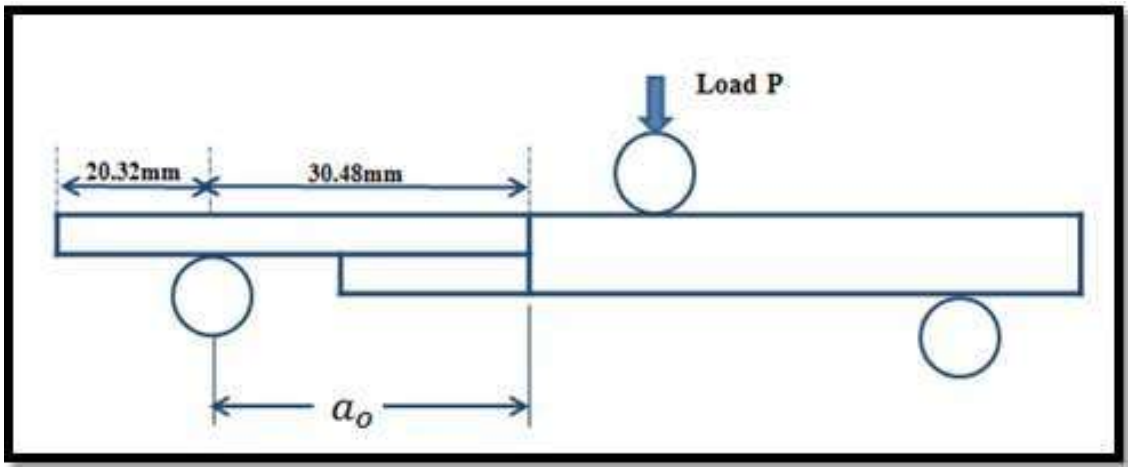

Figure 4.6.5 Single-Leg Bending (SLB) specimen on three points bending flexural for mix mode fracture test marks.

ISSN: 2233-7853IJFGCN

Five mixed-mode samples of each of six designs were tested to calculate G_{Mix-C} mix- mode interlaminar mix-mode (shear and open mode) fracture toughness. Figure 4.6.5. The design is similar to an ENF specimen, but with cut one leg and made shorter than the other by 1.5" (38.1mm). The Instron machine was used to conduct the three point flexural loading. It measured the load and traveling distance. The max load of load cell used was 500 lb. The displacement rate was 0.025 in/min. During the test a magnifier and bright light source were used to follow the crack propagation.

Table 4.6.5
Mix-mode specimen average dimensions

Mode II	Width b	Length L	Thickness h	Initial delamination length a_o
FG-90-V	1.03" (26.22mm)	8" (203.2 mm)	0.177" (4.48mm)	2" (50.8mm)
F.G-90/90	1.032" (26.213mm)	8" (203.2 mm)	0.17" (4.424mm)	2" (50.8mm)
F.G-V/V	1.032" (26.213mm)	8" (203.2 mm)	0.176" (4.486mm)	2" (50.8mm)
CF	1.016" (25.8mm)	8" (203.2 mm)	0.218" (5.54mm)	2" (50.8mm)
H-CF-FG-90 Single-Beam-C.F	1.014" (25.745mm)	8" (177.8mm)	0.181" (4.60mm)	2" (50.8mm)
H-CF-FG-V Single-Beam-C.F	1.02" (25.898mm)	8"(177.8 mm)	0.066" (1.68mm)	2" (50.8mm)
H-CF-FG-90 Single-Beam-FG	1.0636" (27.015mm)	8"(177.8mm)	0.0876" (2.225mm)	2" (50.8mm)
H-CF-FG-V Single-Beam-FG	1.004" (25.5mm)	8"(177.8 mm)	0.088" (2.22mm)	2" (50.8mm)

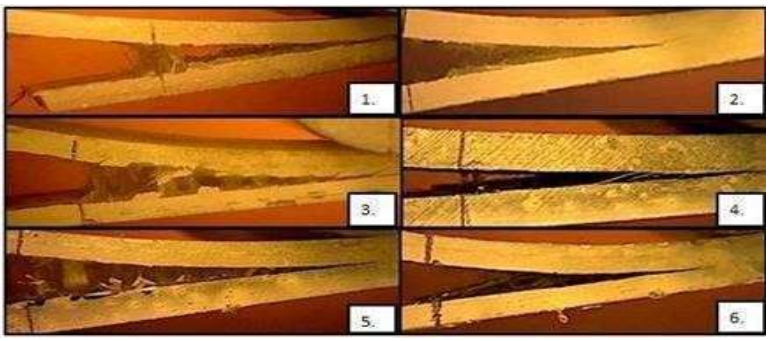

Figure 4.6.6 Mix-mode FG 90/V specimen is on three point flexural. (2)Mix-mode FG V/V specimen is on three points flexural. (3) Mix-mode FG 90/90 specimen is on three points flexural. (4) Mix-mode CF specimen is on three points flexural. (5)H- Mix- mode CF/FG90 specimen is on three points flexural. (6) H- Mix-mode CF/FGV specimen is on three points flexural.

ISSN: 2233-7853IJFGCN

Figure 4.6.6 (1, 3, 5) shows the edges of the specimens under load. The fiber glass 90- V, fiber glass 90-90, and H-CF/FG-90 had fiber bridging. Figure 4.6.6 (4) shows that the carbon fiber fracture moved from layer to another layer. Figure 4.6.6 (2) shows that the fiber glass V-V fracture had little fiber bridging. Figure 4.6.6 (6) hybrid H-CF/ FG V-V had fiber bridging cause by the carbon fiber layers.

5. Results:

1. Mode I Fracture

The summary of the Mode I initiation results are shown in Figure 8.24. The pure carbon fiber composite showed the lowest G_{Ic}. This was followed by 90/90 glass fiber, but at approximately double the value. The next higher results in the all-glass specimens were the V/V specimens; with the highest glass (as well as the highest of all the specimens) were the V/90 specimens. The hybrid specimens, both C-90 and C-V results were similar, and in the range of the all-glass specimens. This is consistent with a visual observation of the fracture surfaces, which showed both faces containing glass. The cracks appeared to propagate in the glass layers of the hybrid specimens. The summary of the Mode I average results are shown in Figure 8.25. Again, the all- carbon specimen had the lowest value of G_{Ic}. This was followed by all-glass V-V specimen. The all-glass V/90 and 90/90 showed much higher values, which is consistent with the extensive fiber bridging observed. The 90/90 showed the most fiber bridging, which is consistent with the fact that it had the highest G_{Ic} value. The two hybrid designs had results in between the all-glass and all-carbon specimens. Additionally, the C/90 showed more fiber bridging than the C/V, and also a higher average toughness. It should be noted that all of the specimen designs containing 90 had the highest toughness values, which was consistent with the extensive fiber bridging observed in specimens with 90 interfaces.

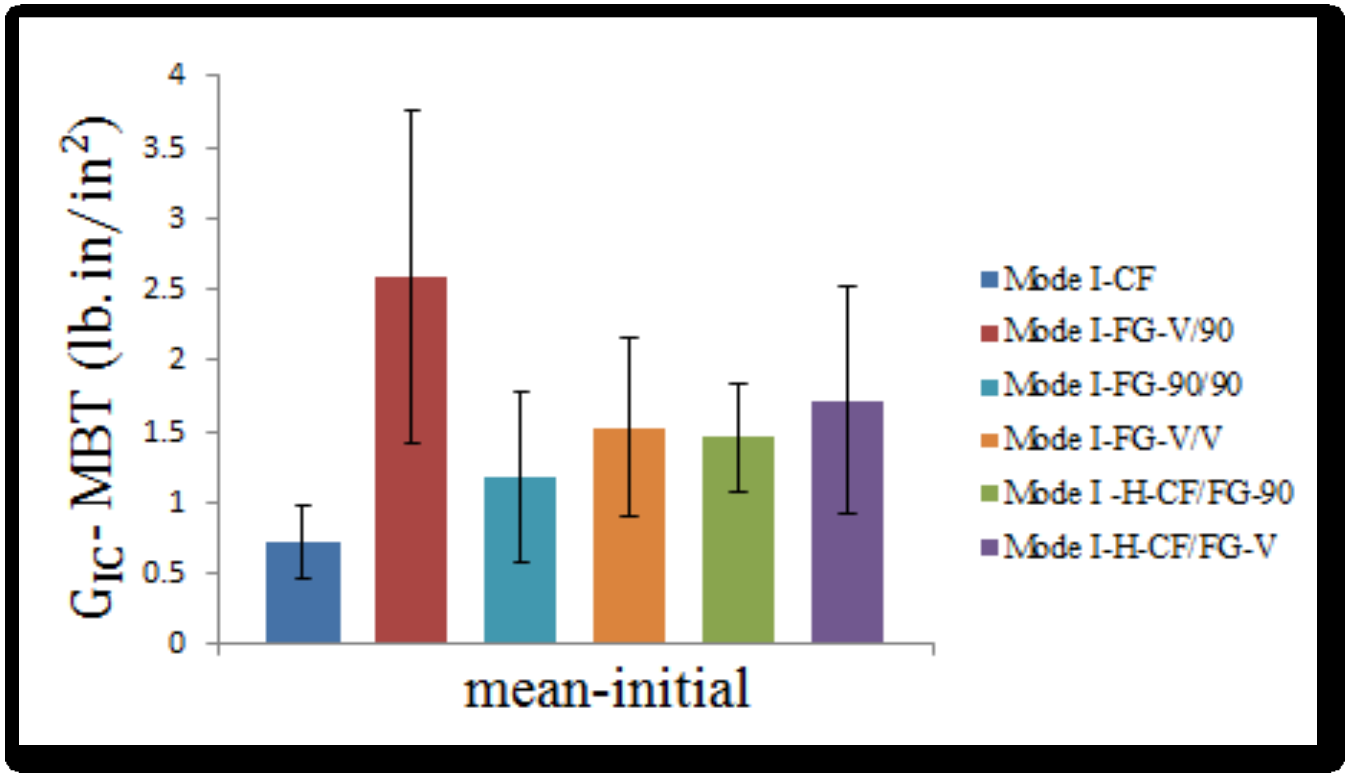

Figure 5.1 Mean initial of mode I strain energy release rate of all mode I specimens by using Modified Beamtheory (MBT).

ISSN: 2233-7853IJFGCN

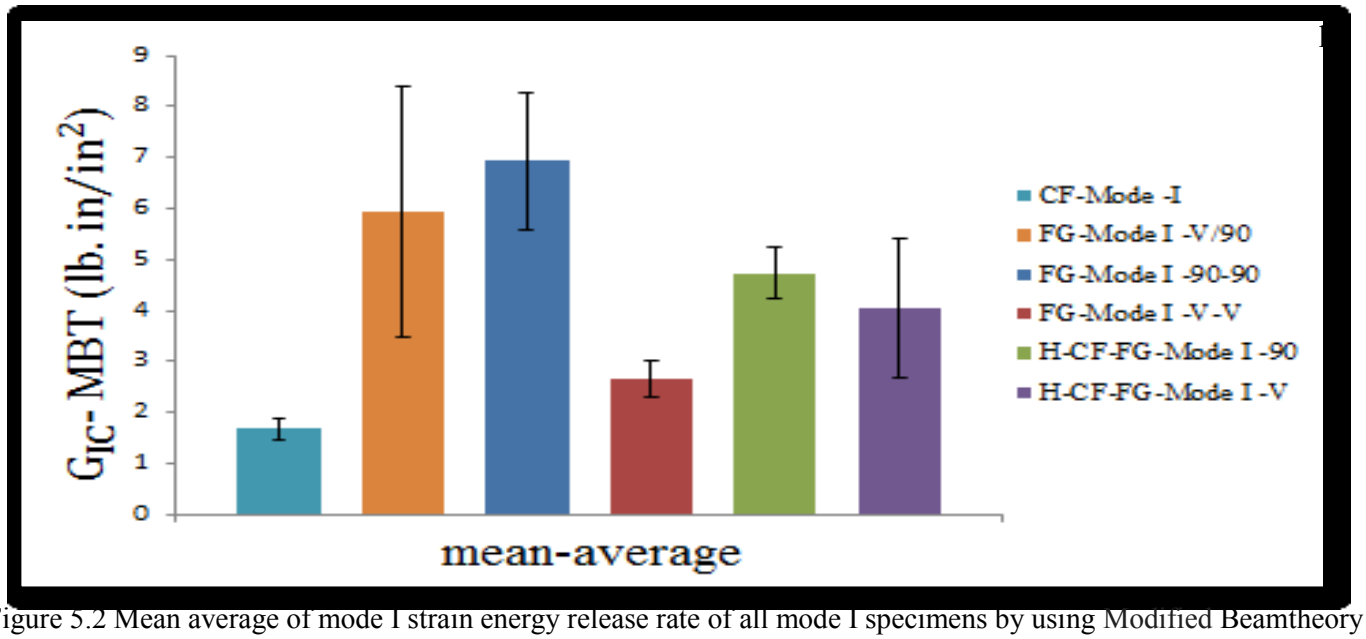

Figure 5.2 Mean average of mode I strain energy release rate of all mode I specimens by using Modified Beamtheory (MBT).

2. Summary of Mode II Fracture

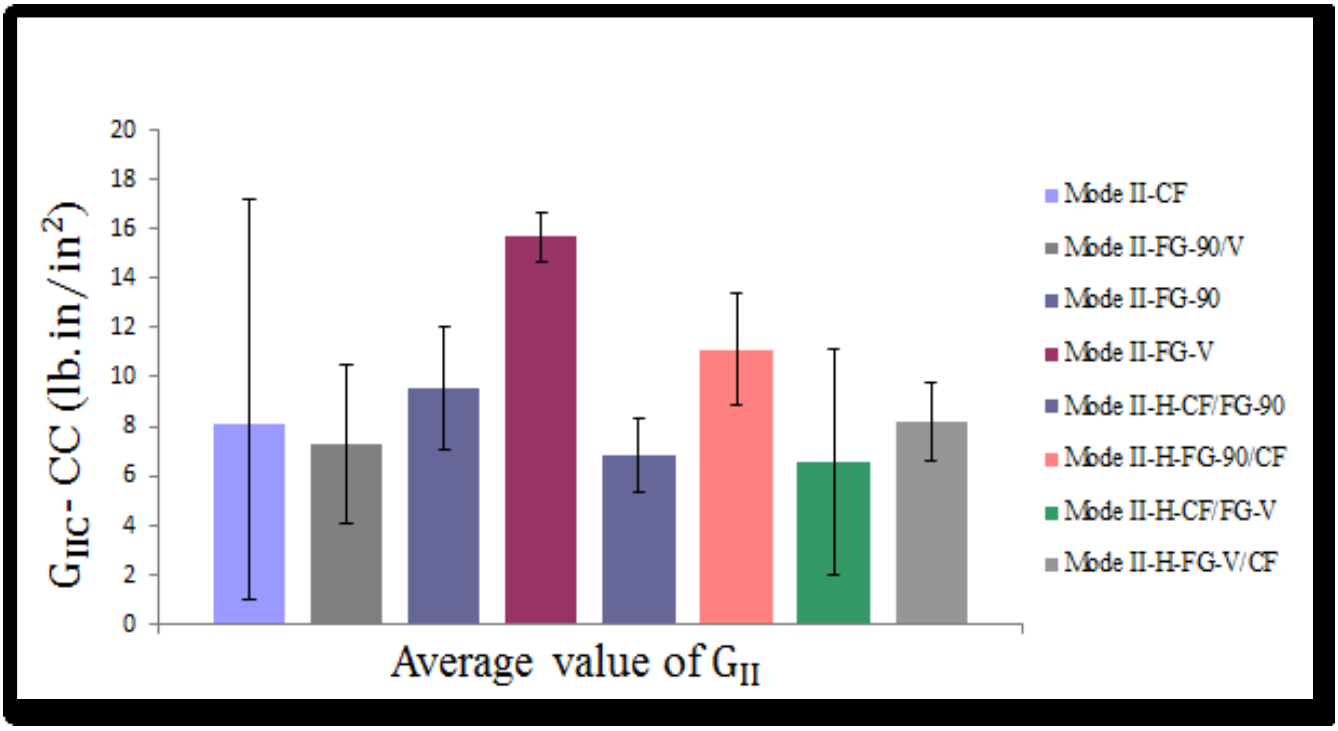

Figure 5.3 Summary"s mode II strain energy release rate of all mode II specimens by using ComplianceCalibration Method.

The summary of the Mode II results can be seen in Figure 8.3.7. The lowest values are for the hybrid specimens tested with carbon fiber as the upper layer. This is followed by the all glass 90/V fracture, then the all-carbon. These values were all similar in value, especially considering the error bands. The next all-glass is the 90/90.

ISSN: 2233-7853IJFGCN

The flipped hybrid specimens follow. Finally the all-glass V/V is the highest. The fiber bridging could not be observed during the test, but could be observed in the scanning electron microscope images, which will be discussed in a later section.

6. Conclusions:

The applications of hybrid composites (such as carbon and glass fiber) materials have been expanding in many fields such as aircraft, wind turbine generators, bridges and infrastructure, sporting goods such as helmets, and marine applications. A composite material may be preferred in applications because of their high strength and stiffness to weight ratio, long fatigue life, and corrosion resistance. In many applications they can be easy to fabricate and offer low cost. [48]. The use of hybrid materials offers the ability for designers to balance the high stiffness and strength of carbon fiber, with the high strength and low cost of glass fiber composites. The present study represents of delamination interface of carbon fiber, fiber glass and hybrid-(fiber glass/carbon fiber) under mode I, mode II and mix-mode I/II static.

The key mechanical test results are summarized in Figures 9.1-9.6.

1. CF and FG-V/V had lowest value of mode I, while FG-90/V and FG-90/90 had the highest values of The H-CF/FG-90 and H-CF/FG-V had values between CF and FG. The H-CF/FG-90 was slightly higher than H-CF/FG-V.
2. FG-V/V had the highest value of The lowest values were from the hybrid H-CF/V specimens.
3. The H-CF/FG-90 was better than H-CF/FG-V in mode II and mixed mode I/II.

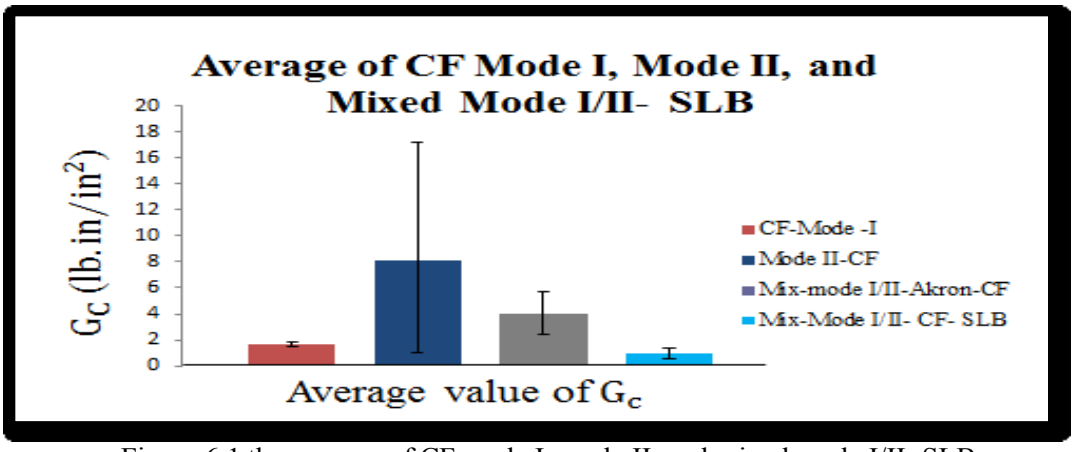

Figure 6.1 the average of CF mode I, mode II, and mixed mode I/II- SLB

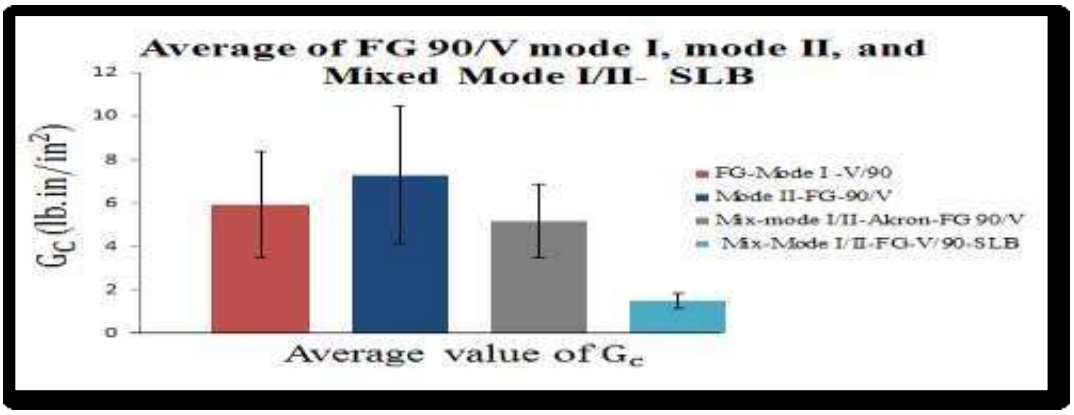

Figure 6.2 the average of FG 90/V mode I, mode II, and mixed mode I/II- SLB

ISSN: 2233-7853IJFGCN

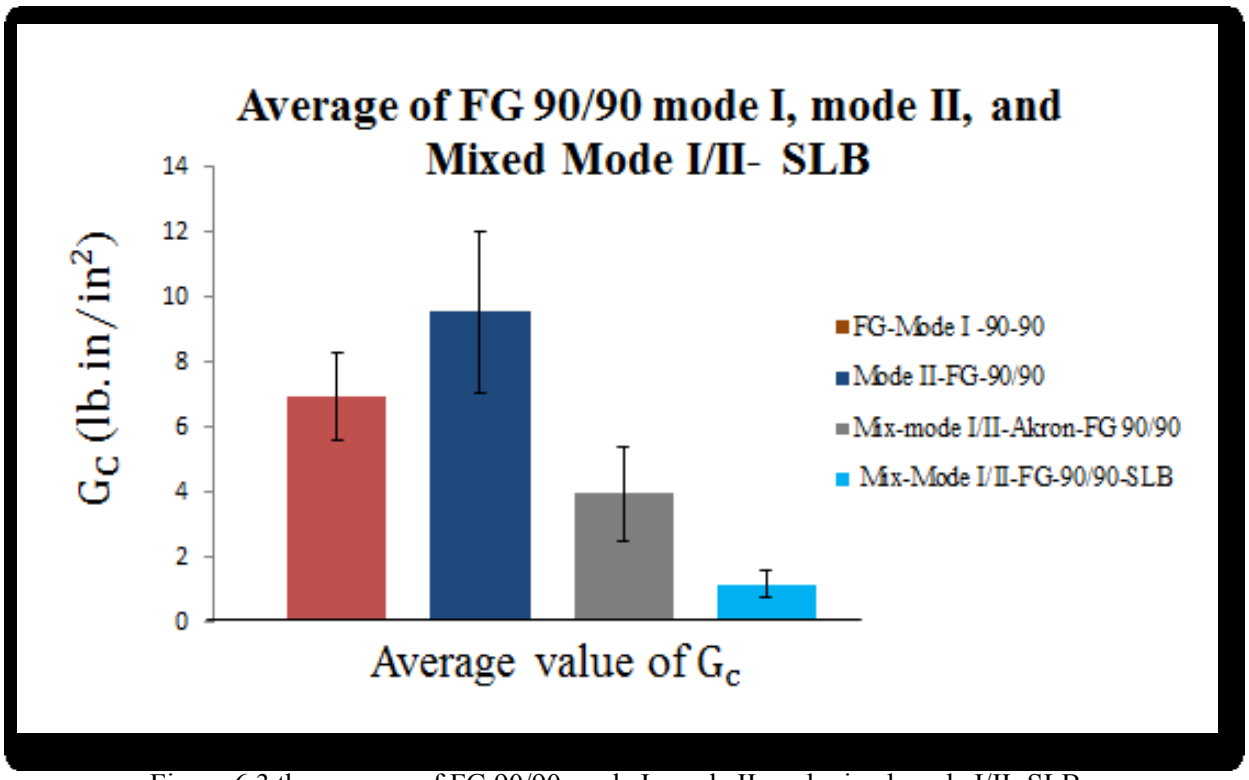

Figure 6.3 the average of FG 90/90 mode I, mode II, and mixed mode I/II- SLB

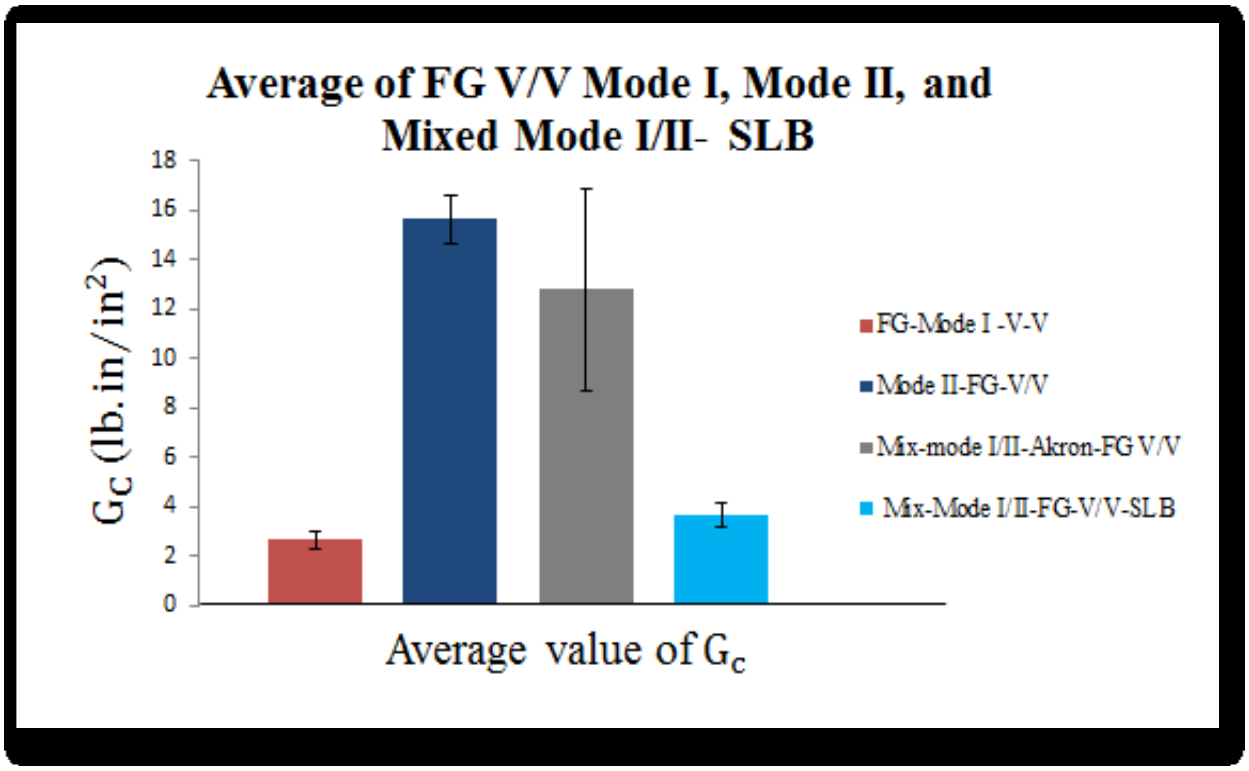

Figure 6.4 the average of FG V/V mode I, mode II, and mixed mode I/II- SLB

ISSN: 2233-7853IJFGCN

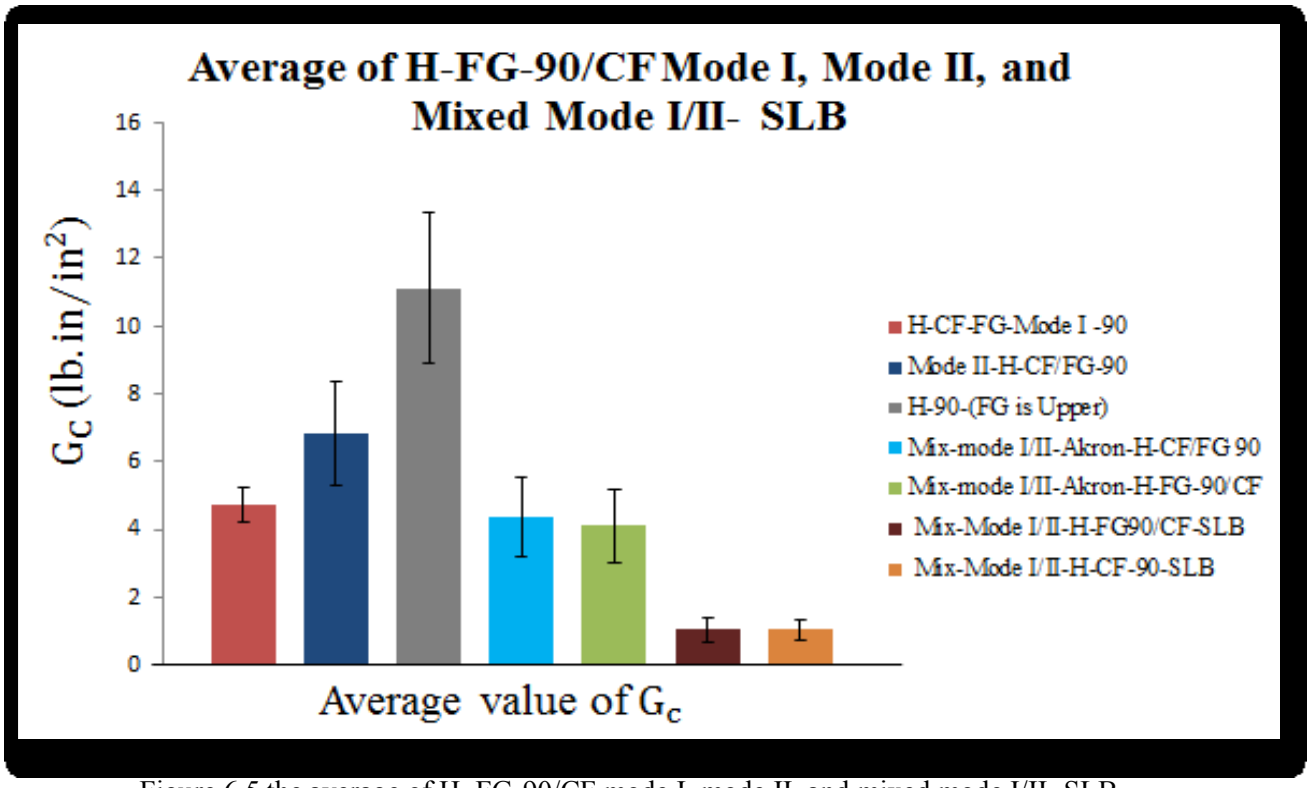

Figure 6.5 the average of H- FG-90/CF mode I, mode II, and mixed mode I/II- SLB

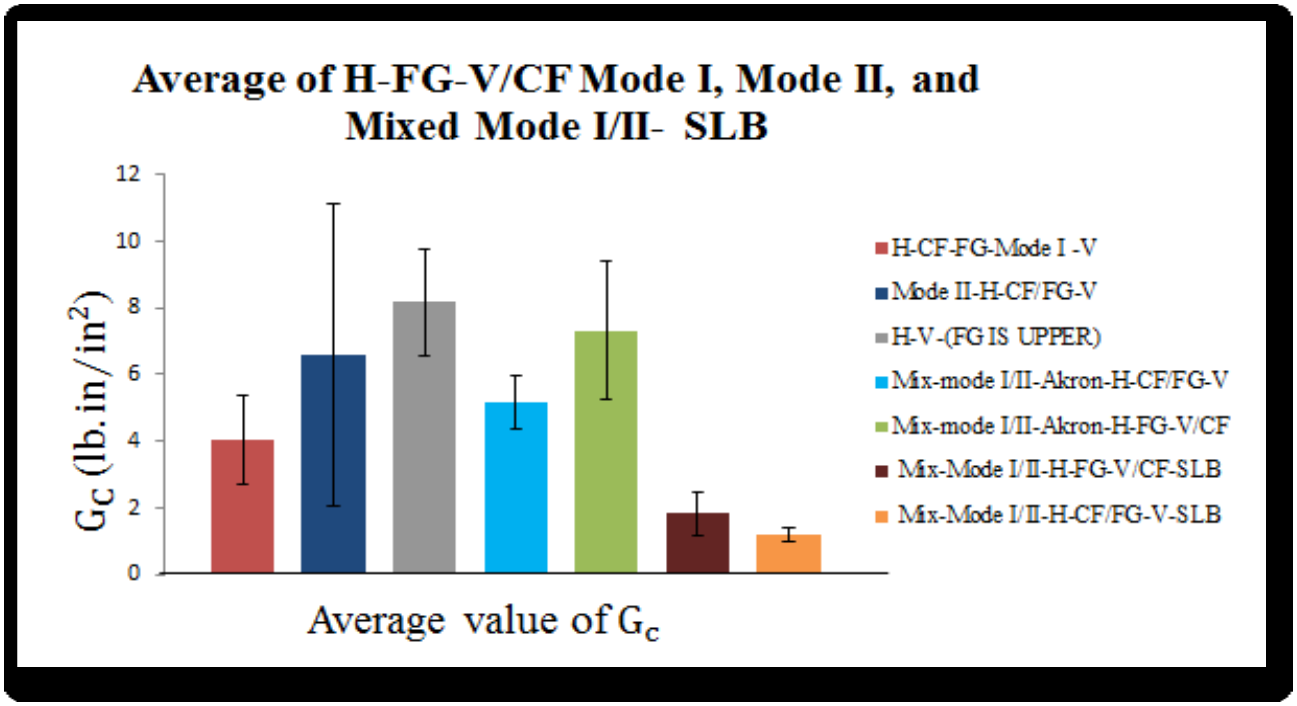

Figure 6.6 the average of H- FG-V/CF mode I, mode II, and mixed mode I/II- SLB

ISSN: 2233-7853IJFGCN

REFERENCES:

1. J.M. Whitney, C.E. Browing and W. Hoogsteden "A Double Cantilever Beam Test for Characterizing Mode I Delamination of Composite Materials" Air Force Wright Aeronautical Laboratories Wright-Patterson, Air Force Base, Ohio 45433, 1982.
2. N. Sela,O. Ishai and L.Banks-Sills ,"The effect of adhesive thickness on interlaminar fracture toughness of interleaved CFRP specimens",1989.
3. A.J. Brunner, B.R.K. Blackman, P. Davies "A status report on delamination resistance testing of polymer–matrix composites" Science Direct, Engineering Fracture Mechanics, 2007.
4. P.N.B. Reis1a, J.A.M. Ferreira, F.V. Antunes, J.D.M. Costa, C. Capela "Analysis of the initial delamination size on the mode I interlaminar fracture of carbon/epoxy composites".
5. Mehdi Barikani, Hossein Saidpour, and Mutlu Sezen. "Mode-I Interlaminar Fracture Toughness in Unidirectional Carbon-fibre/Epoxy Composites".2002.
6. Mohammadreza, Khoshravan, Farhad Asgari Mehrabadi. "Fracture analysis in adhesive composite material/aluminum joints under mode-I loading; experimental and numerical approaches", International Journal of Adhesion & Adhesives, SciVerse Science Direct,2012
7. Moslem Shahverdi, Anastasios P. Vassilopoulos, Thomas Keller "A phenomenological analysis of Mode I fracture of adhesively-bonded pultruded GFRP joints",2011
8. Shun-Fa Hwang, Bon-Cherng Shen. "Opening-mode interlaminar fracture toughness of interply hybrid composite materials".1999.
9. Masahiro Arai, Yukihiro Noro, Koh-ichi Sugimoto, Morinobu Endo "Mode I and mode II interlaminar fracture toughness of CFRP laminates toughened by carbon nanofiber interlayer".Science Direct.Composites Science and Technology.2007.
10. L.F.M. da Silva, V.H.C. Esteves, F.J.P. Chaves "Fracture toughness of a structural adhesive under mixed mode loadings" Mat.-wiss. u.Werkstofftech. 2011, 42,
11. "Fracture Toughness Testing: Part One" http://www.keytometals.com/page.aspx?ID=CheckArticle&site=kts&NM=291
12. Andras Szekre, Jozsef Uj" Comparison of some improved solutions for mixed- mode composite delamination coupons,2005
13. Book of Mechanics of Materials fifth edition by Ferdinand P.Beer, E.Russell Johnston , Jon T. DeWolf, David F. Mazurek
14. Book of engineering mechanics of composite materials second edition by Isaac M. Daniel Ori Ishai
15. ASTM 2734 Method (Epoxy Burn Off)
16. "Wind Energy Composite Materials Handbook from Gurit", accessed 1/18/2013, 2013, http://www.gurit.com/wind-energy-hand-book.aspx.
17. "Design News - Features - Sandia Sizes up Wind Turbine Blade Design ", accessed 1/18/2013,
18. http://www.designnews.com/document.asp?doc_id=230008&dfpPParams=ind_182,aid_230008&dfpLayout=article.
19. Mansour H. Mohamed, Kyle K. Wetzel, "3D Woven Carbon/Glass Hybrid Spar Cap for Wind Turbine Rotor Blade", Journal of Solar Energy Engineering NOVEMBER 2006, Vol. 128
20. W.C. de Goeij, M.J.L. van Tooren, A. Beukers "Implementation of bending- torsion coupling in the design of a wind-turbine rotor-blade", Applied Energy 63 (1999) 191-207

ISSN: 2233-7853IJFGCN

21. Dayton A. Griffin, Global Energy Concepts, LLC , 5729 Lakeview Drive NE, #100 ,Kirkland, Washington 98109 "Blade System Design Studies Volume I: Composite Technologies for Large Wind Turbine Blades"
22. John F. Mandell,Douglas S. Cairns,Daniel D. Samborsky, Robert B. Morehead and Darrin H. Haugen "Prediction of Delamination in Wind Turbine Blade Structural Details", ASME 2003 Wind Energy Symposium
23. Paul S. Veers,Thomas D. Ashwill, Herbert J. Sutherland, Daniel L. Laird and Donald W. Lobitz, John F. Mandell, Walter D. Musial, Kevin Jackson, Michael Zuteck, Antonio Miravete, Stephen W. Tsai, James L. Richmond, "Trends in the Design, Manufacture and Evaluation of Wind Turbine Blades", Wind Energ. 2003; 6:245–259 (DOI: 10.1002/we.90)
24. Cheng Ong,Design, manufacture and testing of a bend-twist D-spar", 1999 http://arc.aiaa.org/doi/abs/10.2514/6.1999-25

ISSN: 2233-7853IJFGCN